Water Resources Research

REVIEW ARTICLE
10.1029/2025WR043172

Special Collection:
Celebrating the 60th Anniversary of Water Resources Research

The Evolving Roles of Electrical Geophysical Methods for In Situ Remediation Assessment: Progress and Perspectives

Teng Xia[1,2], Miao Li[1], Lee Slater[3], Xiangyun Hu[4], Andrew Binley[5], Xinmin Ma[6], and Deqiang Mao[2]

[1]School of Environment, Tsinghua University, Beijing, China, [2]School of Civil Engineering, Shandong University, Jinan, China, [3]Department of Earth and Environmental Sciences, Rutgers University Newark, Newark, NJ, USA, [4]Institute of Geophysics and Geomatics, China University of Geosciences, Wuhan, China, [5]Lancaster Environment Centre, Lancaster University, Lancaster, UK, [6]School of Earth Sciences and Engineering, Hohai University, Nanjing, China

Abstract In situ remediation of contaminated soil and groundwater demands real-time monitoring to capture complex subsurface dynamics. Geophysical methods, particularly electrical resistivity tomography (ERT) and induced polarization (IP), offer non- or minimally invasive, high-resolution imaging of subsurface changes during remediation. This is the first review to synthesize advances in geophysical monitoring of four key technologies: in situ chemical oxidation/reduction (ISCO/ISCR), in situ bioremediation (ISB), in situ thermal remediation (ISTR), and permeable reactive barriers (PRB). We systematically examine how variations in hydrogeology, temperature, hydrochemistry and contaminant indicators influence electrical responses, and discuss the principles, advantages, and limitations of ERT/IP for each technology. Based on a bibliometric analysis of over 200 studies, we identify current trends, critical challenges, and future research directions. Integrating geophysical methods with direct sampling is essential to transform electrical signatures into actionable insights for remediation management. Continued progress will be made via advances in petrophysical relationships, multi-source data fusion coupled inversion frameworks, and the application of artificial intelligence and machine learning approaches to enable real-time, adaptive remediation strategies.

Plain Language Summary Soil and groundwater contaminated by industrial activity threaten ecosystems and human health. Clean-up of these sites via remediation technologies is critical, but tracking remediation progress and effectiveness in real time remains difficult. Traditional well sampling provides only point-specific data and can miss heterogenous subsurface changes. This review synthesizes two decades of research showing how electrical geophysical methods, specifically electrical resistivity tomography and induced polarization, serve as effective remediation monitoring tools. By imaging changes in electrical properties of the subsurface, these techniques indirectly track heat distribution, reagent migration, and contaminant breakdown during chemical oxidation, bioremediation, thermal treatment, and permeable reactive barrier applications. We discuss current challenges and future opportunities to integrate geophysics with direct sampling, that will ultimately enable more adaptive and sustainable remediation strategies.

Key Points:

- Targets the shallow subsurface key to groundwater and ecosystem resilience
- Electrical parameters indicate subsurface changes during remediation
- Integrating multi-source data improves insight for optimizing remediation strategies

Supporting Information:

Supporting Information may be found in the online version of this article.

Correspondence to:

D. Mao,
maodeqiang@sdu.edu.cn

Citation:

Xia, T., Li, M., Slater, L., Hu, X., Binley, A., Ma, X., & Mao, D. (2026). The evolving roles of electrical geophysical methods for in situ remediation assessment: Progress and perspectives. *Water Resources Research*, *62*, e2025WR043172. https://doi.org/10.1029/2025WR043172

Received 18 DEC 2025
Accepted 7 APR 2026

Author Contributions:

Conceptualization: Teng Xia, Deqiang Mao
Formal analysis: Teng Xia, Miao Li, Lee Slater, Andrew Binley
Funding acquisition: Teng Xia, Deqiang Mao
Investigation: Xinmin Ma
Methodology: Teng Xia, Lee Slater, Xiangyun Hu, Andrew Binley, Xinmin Ma
Resources: Deqiang Mao
Writing – original draft: Teng Xia
Writing – review & editing: Miao Li, Lee Slater, Xiangyun Hu, Andrew Binley, Deqiang Mao

1. Introduction

Soil and groundwater are indispensable natural resources that sustain life and ecosystems (Scanlon et al., 2023). However, human activities such as industrial activity, agriculture and waste disposal have introduced harmful contaminants into soil and groundwater, including non-aqueous phase liquids (NAPLs), heavy metals, radioactive wastes, etc (Elshall et al., 2020; Karandish et al., 2025). The remediation of contaminated soil and groundwater is therefore essential to safeguard human health, protect ecosystems, and ensure the sustainable use of resources (Hou & O'Connor, 2020).

Treatment of subsurface contaminants can be categorized as ex situ or in situ remediation (Hussain et al., 2022). Ex situ remediation consists of excavating soil or pumping groundwater from the aquifer and then remediating it with appropriate facilities on the surface (Zhang, Labianca, et al., 2021). This approach is characterized by high energy and chemical consumption, the risk of contaminant dispersion, and significant disturbance of the soil or aquifer (Shao et al., 2025). *In situ* remediation, in contrast, can complete the remediation of a contaminated plume whilst overcoming these drawbacks as it allows for direct treatment at contaminated sites (Wang et al., 2025; Yuan et al., 2024). Experiments and technology demonstrations conducted across both field and laboratory scales

have consistently validated the effectiveness of these technologies for removing contaminants within soil and groundwater (e.g., Marcon et al., 2021; Song et al., 2017; Zhao et al., 2022).

Within the United States, an analysis of Superfund remediation records (EPA, 2023) shows that 47% of the 118 soil and groundwater remediation projects implemented from 2018 to 2020 used in situ technologies, with bioremediation (25%), chemical treatment (16%) and thermal treatment (9%) being the most selected. Additionally, the permeable reactive barrier (PRB) technology, widely used in groundwater remediation, combining passive chemical or biological treatment zones with groundwater flow, accounted for 3% during the same time period. Bioremediation, chemical treatment, and PRBs are recognized for substantially reducing the environmental footprint of remediation whilst maximizing net benefits, owing to their technological maturity and previous life-cycle assessments (Hou et al., 2023).

This review focuses on four key technologies from the perspective of treatment processes (Figure 1): in situ thermal remediation (ISTR), in situ chemical oxidation/reduction (ISCO/ISCR), in situ bioremediation (ISB) and PRBs. ISTR is one of the most effective ways to deal with significant source areas (particularly NAPLs) in a reasonable timeframe (Horst et al., 2021). This method employs controlled subsurface heating (typically 60–400° C) via resistive heating or steam injection to enhance contaminant mobility and removal. Precise monitoring of heat transfer coverage and energy consumption is therefore required (Colombano et al., 2020; Davis, 2023). ISCO/ISCR utilizes injected oxidants (e.g., persulfate) or reductants (e.g., zero-valent iron (ZVI)) to degrade contaminants through redox reactions. Particular attention is paid to reagent transport pathways and radius of influence (Flores Orozco et al., 2015; Wei et al., 2022). In contrast, ISB stimulates microbial activity by adding nutrients or microbial communities to enhance biological degradation. Its effectiveness is primarily determined by microbial reactivity (Griffiths, 2020; Romantschuk et al., 2023). PRBs passively intercept and treat contaminant plumes using reactive materials (e.g., zero valent iron (ZVI)), primarily through adsorption or chemical reaction. Hydraulic properties of the aquifer and material reaction longevity are critical parameters controlling PRB effectiveness (Budania & Dangayach, 2023; Mak & Lo, 2011).

While the above technologies utilize different remediation mechanisms, their deployment consistently triggers multi-scale interactions. These can encompass subsurface changes in temperature, fluid flow, solute transport, biochemical interactions, and contaminant removal (Grotenhuis & Rijnaarts, 2011; Padhye et al., 2023). Hydrogeological conditions, hydrochemistry and biological environment, contaminant type and concentration, remediation materials and remediation strategies all affect the performance of subsurface remediation processes (Tratnyek et al., 2014; Wang et al., 2021). These complex and multi-scale interactions during in situ remediation must be accurately captured in real time. Otherwise, our ability to understand, evaluate, and ultimately sustainably adapt remediation strategies is restricted.

Conventional monitoring relies on sampling from wells, which provides accurate point measurements but faces inherent limitations. Concentrations from monitoring wells reflect treatment across the aquifer (Lévy et al., 2024), while low spatial sampling density may not capture vertical contaminant dispersion and risk uncertain interpolation of discontinuous stratigraphic data (Xia, Meng, et al., 2023). These constraints impede characterization of reagent transport pathways in ISCO/ISCR, microbial reactivity zones in ISB, heat transfer coverage in ISTR, and hydraulic property evolution in PRBs. Consequently, real-time processes involving multi-scale interactions such as subsurface heating, fluid flow, reactive transport, biochemistry, and contaminant removal cannot be fully captured.

These limitations have promoted the adoption of electrical geophysical techniques, particularly electrical resistivity tomography (ERT) and induced polarization (IP) (Binley & Slater, 2020). These methods have emerged as valuable tools for providing continuous spatial information between individual boreholes during remediation (Alao et al., 2024; Day-Lewis et al., 2017; LaBrecque et al., 1996). ERT is an electrical imaging technique that can be deployed in surface or cross-borehole configurations. It monitors changes in electrical resistivity (or electrical conductivity, its inverse) during remediation progress. This method involves injecting a known current into the ground through two electrodes and recording the potential difference between another pair of electrodes (Dahlin & Loke, 2018). The resulting measurements reflect electrical conduction processes in the subsurface medium. Induced polarization extends ERT by simultaneously characterizing both the conductive and charge storage properties of the subsurface. IP can improve the mapping of lithological variations, the estimation of permeability distributions, and the characterization of pore-fluid interactions (Slater & Lesmes, 2002). For example, Almpanis et al. (2021) employed a novel DNAPL-DCIP model and confirmed that resistivity effectively

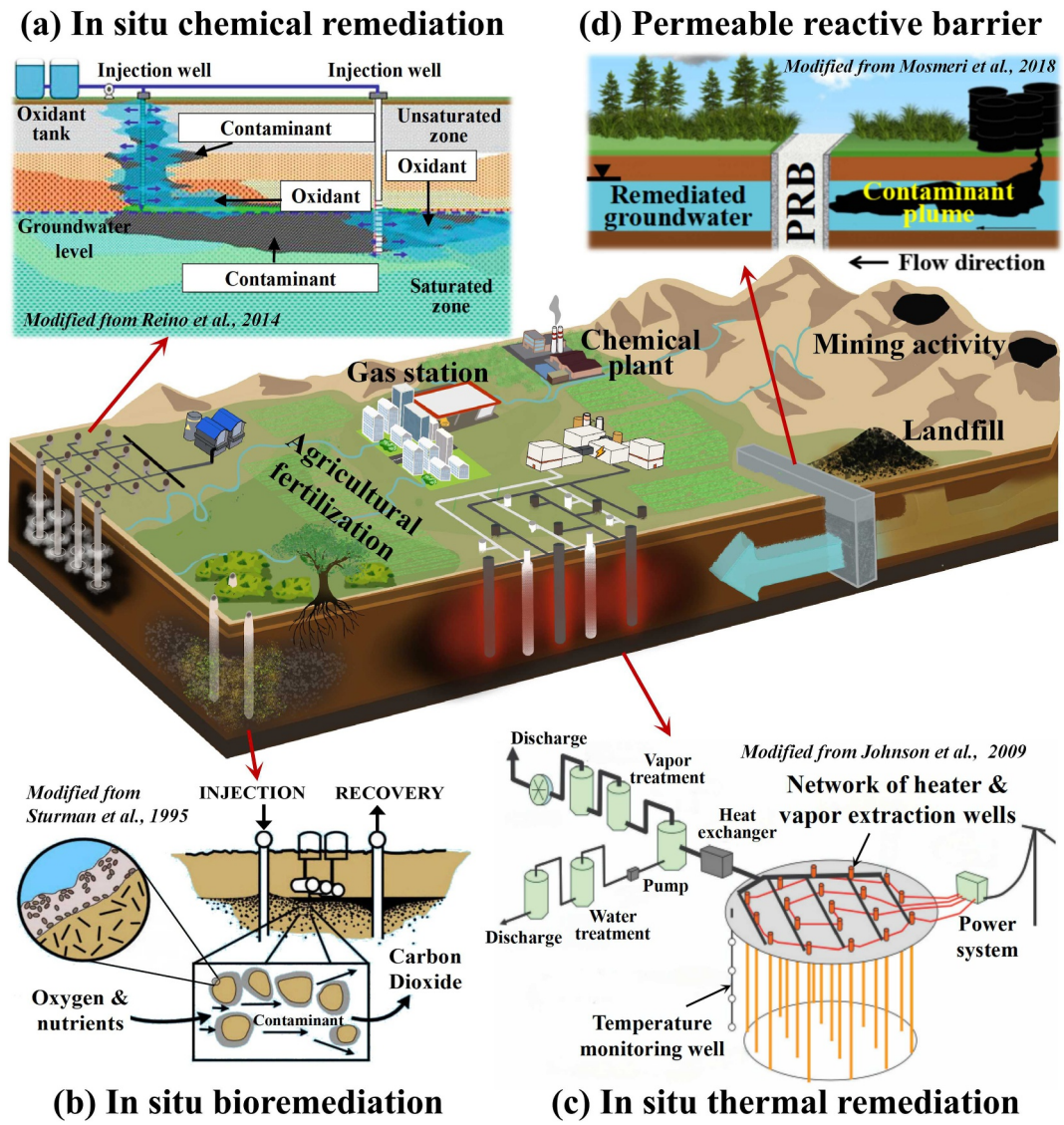

Figure 1. Conceptual model showing in situ remediation strategies. (a) In situ chemical remediation (ISCO/ISCR) uses injected oxidants or reductants to degrade contaminants via redox reactions. (b) In situ bioremediation (ISB) enhances biological degradation by stimulating native microbial activity with nutrient amendments. (c) In situ thermal remediation (ISTR) improves contaminant mobility and removal through controlled subsurface heating using resistive heating or steam injection. (d) Permeable reactive barrier (PRB) passively treats contaminant plumes using reactive materials for adsorption or chemical reduction.

tracks DNAPL mass reduction, while chargeability (a measure of charge storage) aids in delineating the subsurface lithology governing DNAPL distribution.

Time-lapse electrical imaging has proved to be a highly effective method for tracking temporal changes in subsurface electrical parameters. These changes often reflect variations in fluid saturation, contaminant concentration, temperature, and pore fluid composition. Such variations result from processes including heating, fluid migration, degradation, and biochemical reactions during in situ remediation (Kemna et al., 2012; Martinho, 2023; Singha et al., 2014; Tildy et al., 2017). However, electrical geophysical monitoring alone cannot directly quantify remediation effectiveness. Geophysical techniques should be integrated with direct measurement information, particularly samples from monitoring wells, to establish relationships between electrical properties and key indicators. These include hydrogeological, thermal, hydrochemical, and contaminant indicators. Such integration is key to enabling real-time assessment of remediation progress and guiding strategy

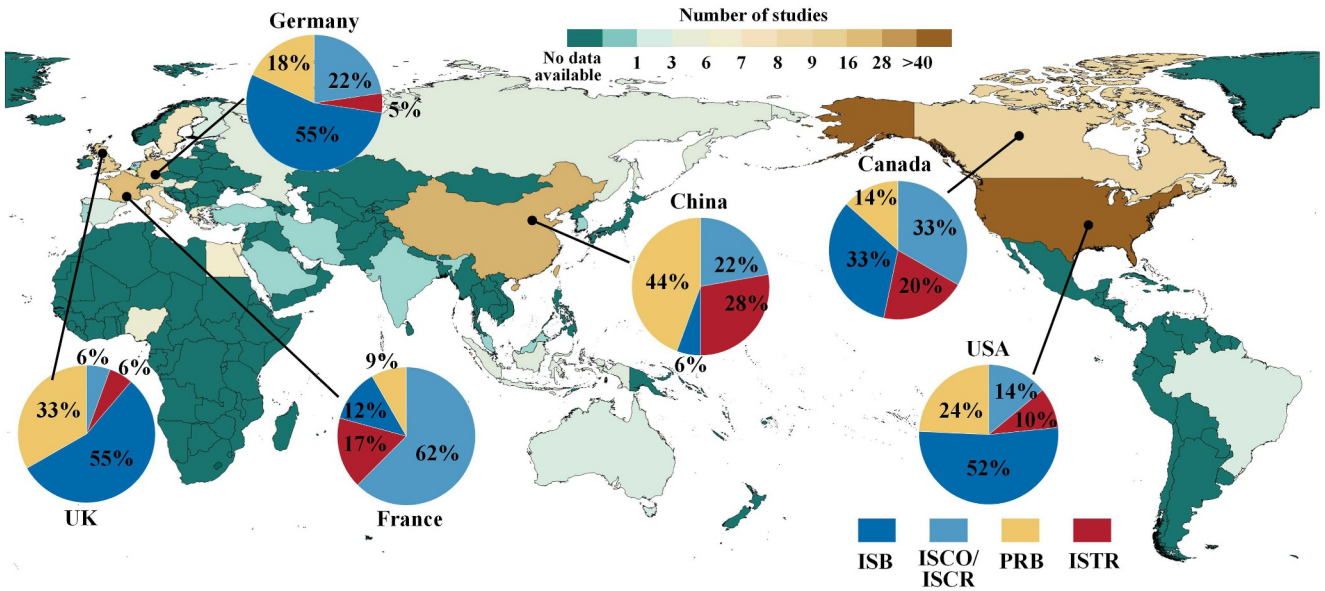

Figure 2. Number of studies by country and their focus on electrical geophysical monitoring of in situ remediation processes. The figure illustrates the distribution of in situ remediation strategies adopted by the six leading countries.

optimization (Binley et al., 2015; Kessouri et al., 2022; Thompson et al., 2023). A deep understanding of these relationships is thus essential for advancing the application of geophysical monitoring during in situ remediation.

While previous studies have examined geophysical monitoring of remediation technologies or focused on methodological aspects of ERT/IP, a synthesis that systematically compares how electrical signatures manifest across different treatment mechanisms remains lacking. This review addresses this gap by providing the first cross-technology framework that (a) compares how thermal, chemical, biological, and permeable barrier remediation processes distinctly influence electrical properties, (b) establishes how multi-scale subsurface interactions collectively govern these geophysical responses, and (c) outlines a roadmap for transforming geophysical data into actionable remediation insights through integration with direct sampling. By synthesizing geophysical monitoring advances across ISCO/ISCR, ISB, ISTR, and PRB technologies, we provide a novel perspective that enables comparative understanding of how ERT/IP can be applied across these diverse remediation approaches.

To elucidate research trends in electrical-based monitoring of remediation processes, we conducted a bibliometric analysis of academic research conducted at field and laboratory scales. As evidenced by the 209 studies analyzed (see Supporting Information S1), research in this field is geographically broadly distributed (Figure 2). Literature analysis reveals that researchers across 30 countries have employed electrical geophysical methods to monitor ISCO, ISB, ISTR, and PRB remediation technologies. The United States (114 publications), China (36), France (27), Germany (25), United Kingdom (24), and Canada (21), constitute the primary contributors, while other nations each produced fewer than 20 studies. Among these technologies, ISB dominates geophysical monitoring applications, representing nearly half of U.S. geophysical remediation research. Figure 3 further quantifies this distribution: ISB accounts for 46% of applications, followed by ISCO/ISCR (21%), PRB (20%), and ISTR (13%). Field-scale studies comprise 49% of total investigations versus 51% for laboratory studies. Specifically, ISCO/ISCR and ISTR monitoring occurs more frequently in field settings, whereas ISB and PRB applications predominantly feature laboratory-scale investigations.

Building on these statistics, we review advances in geophysical monitoring of ISCO/ISCR, ISB, ISTR, and PRB remediation across field and laboratory scales. We summarize key factors influencing electrical properties during remediation. The principles, advantages, and limitations of ERT/IP are systematically addressed for each remediation technology considered. Finally, we identify critical challenges and future research directions to enhance the efficacy of remediation monitoring.

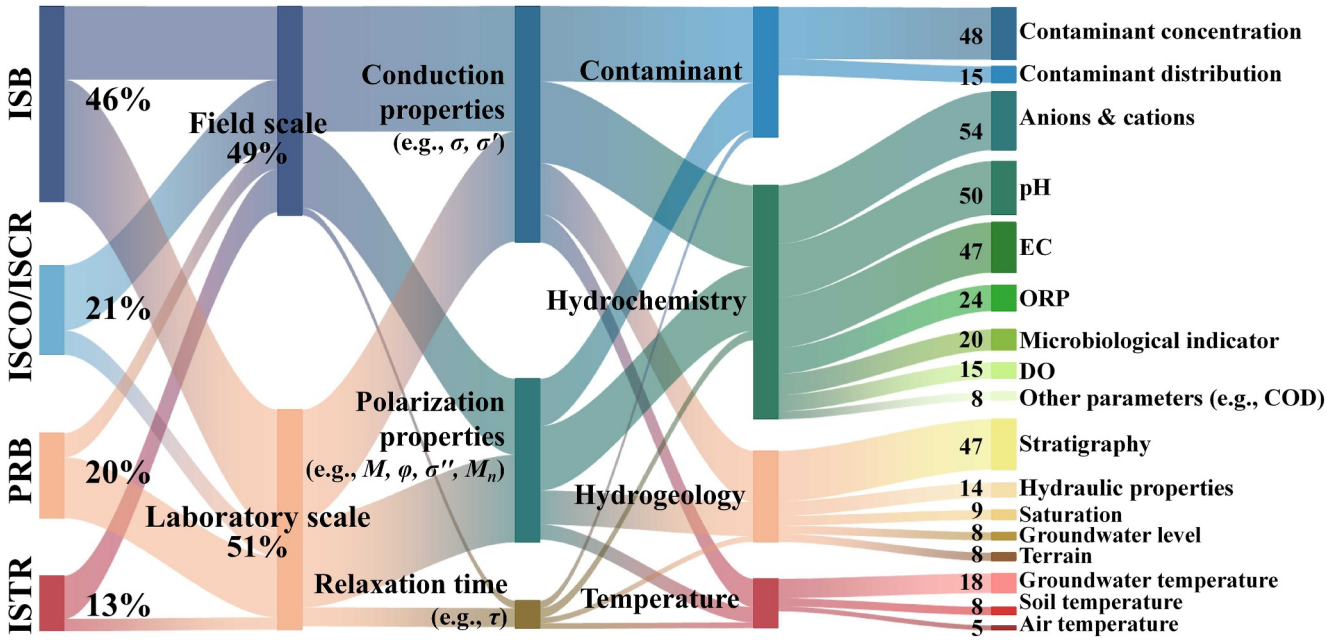

Figure 3. Factors affecting electrical properties during in situ remediation. The statistics are based on the frequencies mentioned in the literature. Key electrical parameters comprise three categories: Conduction properties (e.g., conductivity σ, real conductivity σ'), polarization properties (chargeability M, phase φ, imaginary conductivity σ'', normalized polarizability M_n), and time constants (e.g., relaxation time τ). Beyond electrical properties, key monitoring parameters include four factors: hydrogeology, temperature, hydrochemistry, and contaminant type.

2. Electrical Geophysical Methods

2.1. Definitions of ERT and IP

A range of geophysical methods have been extensively used in the field of environmental investigations. In terms of geophysical monitoring of in situ remediation process, we restrict this review to the general concepts of electrical geophysical methods, that is, ERT and IP. These methods are selected for their remarkable adaptability across both short and long spatial and temporal scales (Slater & Binley, 2021). The key advantages of these approaches are twofold: (a) the instrumentation is adaptable for semi-permanent to permanent installations, enabling robust long-term monitoring, and (b) the resulting time-lapse measurements are particularly sensitive to changes in subsurface properties influenced by remediation techniques. These capabilities are seldom achieved with other geophysical methods.

ERT measures variations in the subsurface resistivity distribution by employing an array of electrodes. Resistivity quantifies how strongly a material resists the transport of electric charges. It is highly sensitive to changes in subsurface conditions such as fluid content, salinity, and lithology, thereby providing insights into hydrogeological and geotechnical properties. Measurements can be made using various electrode array configurations, each offering distinct sensitivity distributions and depth of investigation (Telford et al., 1990). The commonly used electrode arrays in ERT include the Wenner, Schlumberger, Dipole-Dipole, and Gradient configurations, among others (e.g., Alao et al., 2024; Binley & Slater, 2020). The selection of a specific array is generally determined by the survey objectives, the nature of the target, and occasionally the versatility of the instrument. Modern computer-controlled multi-electrode systems offer the capability to readily optimize the survey array by combining different configurations. This should be considered during the survey design stage. The intrinsic electrical properties of porous media can be described in terms of either the resistivity or the conductivity (the inverse of resistivity); here we adopt conductivity, σ, as the preferred parameter.

To image the conductivity distribution in a heterogeneous subsurface, inversion of the ERT data is required (Loke & Barker, 1996). Inversion, in this context, is a numerical process that determines the distribution of electrical conductivity i.e. consistent with the observed set of ERT data. Without constraints, the inverse problem may suffer from non-uniqueness as there are typically many more parameters to estimate than measurements acquired. Inversions may also suffer from convergence problems due to model and data errors. To obtain a stable and

geologically plausible solution that honors data quality subject to noise levels, regularization (e.g., spatial constraints and/or the incorporation of a priori information in the model or data space) is therefore required during the inversion process (Binley & Slater, 2020). ERT data can be analyzed as a single "shapshot" of the subsurface whereas, in contrast, time-lapse imaging allows the recovery of sequence of images of the subsurface at specific times (e.g., Karaoulis et al., 2011). Such analysis reflects changes in the subsurface electrical conductivity distribution at a temporal resolution primarily determined by the time required to acquire a single data set. In order to reconstruct reasonable, smooth changes in conductivity over time, time-lapse inversion techniques can be employed using temporal regularization, for example between pairs of ERT data sets or across multiple inversions (e.g., Kim et al., 2009; Miller et al., 2008). Each time-lapse inversion method has its own distinct advantages and limitations, making the selection of an optimal approach dependent on the specific application (Singha et al., 2014). For example, simultaneous inversion methods that consider multiple data sets (e.g., Hayley et al., 2011; Karaoulis et al., 2011) are flexible and theoretically sound, but they are often computationally intensive and may be impractical for large-scale inverse problems. In contrast, the analysis of pairs of data, for example, constraining changes in electrical conductivity relative to a reference case, such as in the difference inversion approach of LaBrecque and Yang (2001), is computationally efficient. However, it relies on the assumption that temporal changes in electrical conductivity are sufficiently small to allow the use of a single, consistent sensitivity matrix across all time-lapse inversion steps.

IP instruments survey in either the frequency domain or time domain. The parameters obtained from these measurements reflect the conductive and capacitive properties of the subsurface. In the frequency domain, the IP signal can be presented as the amplitude ratio (σ||) and phase shift (φ) between recorded voltage and injected current waveforms. The complex conductivity σ^* is commonly used to describe frequency domain measurements,

$$\sigma^*(\omega) = |\sigma| e^{i\varphi} = \sigma' + i\sigma'', \tag{1}$$

where $\omega = 2\pi f$ is angular frequency (rad), f is frequency (Hz), $i = \sqrt{-1}$ represents the pure imaginary number, $|\sigma|$ is the magnitude of electrical conductivity (S/m) and φ is phase (rad). The real component (σ') of the complex conductivityrepresents energy loss through conduction, while the imaginary component (σ'') represents reversible energy storage associated with polarization (i.e., delayed charge accumulation and release). The real and imaginary conductivity are related to the magnitude and phase by:

$$|\sigma^*(\omega)| = \sqrt{\sigma'^2 + \sigma''^2}, \tag{2}$$

$$\varphi = \tan^{-1}(\sigma''/\sigma'). \tag{3}$$

In the time domain, the magnitude of the IP effect is described by the chargeability M (Seigel, 1959):

$$M = \frac{V_s}{V_p}, \tag{4}$$

where V_s (V) is the maximum voltage measured immediately after the interruption of a long current pulse and V_p (V) is the primary voltage of the transmitted direct current. Although unitless, it is common practice to report M with the units of mV/V. In practice, however, V_s cannot be directly measured due to the need for a short "dead time" following current shutoff to avoid electromagnetic coupling effects. Therefore, the intrinsic maximum chargeability is not directly measurable and must be estimated by fitting of the measured decay curve (e.g., Florsch et al., 2011).

Spectral induced polarization (SIP) refers to the measurement of the frequency dependence of complex conductivity, with the primary goal of extracting additional information on the physicochemical properties of porous media from their characteristic frequency responses (Kemna et al., 2012). Frequency-dependent IP measurements provide not only a measure of polarization strength but also the characteristic relaxation time τ, provided adequate spectral coverage of the measurements is made. This fundamental parameter represents the dominant time scale of the polarization process.

Relaxation models are commonly represented in terms of an effective complex conductivity. The commonly used Cole–Cole expression (Cole & Cole, 1941), originally defined for a complex dielectric permittivity, can be expressed in terms of complex conductivity,

$$\sigma^*(\omega) = \sigma_\infty - \frac{\sigma_\infty - \sigma_0}{1 + (\mathrm{i}\omega\tau_0)^c}, \tag{5}$$

where $\sigma^*(\omega)$ is the modeled complex conductivity, σ_∞ and σ_0 are the high and low frequency values of conductivity magnitude, $\sigma_\infty - \sigma_0$ quantifies the strength of polarization, τ_0 is directly related to the critical frequency defined as the peak in imaginary conductivity, and c is an exponent describing the steepness of the dispersion. Note that another formulation, often referred to as the Pelton model (Pelton et al., 1978), expresses the complex resistivity $\rho^*(\omega)$ in an analogous form. While both are commonly called "Cole-Cole models" in the geophysics literature, they yield different values for the relaxation time when fitted to the same data. This discrepancy arises as the Cole-Cole relaxation time is the inverse of the imaginary conductivity peak frequency, while the Pelton-Cole relaxation time is the inverse of the imaginary resistivity peak frequency. For high chargeabilities, these peak frequencies differ substantially. A detailed comparison of the two formulations and their implications for data interpretation is provided by Tarasov and Titov (2013).

2.2. Conduction and Polarization Processes in Subsurface Media

In the absence of conductive minerals, charge transport occurs predominantly through ion migration within the medium. In this case, the total conductivity (σ) of a porous medium is often represented as the parallel addition of the electrolytic conductivity (σ_{el}) and the interface-related conductivity (σ_{surf}) (Binley & Slater, 2020),

$$\sigma = \sigma_{el} + \sigma_{\mathrm{surf}} = \frac{\sigma_w}{F} + \sigma_{\mathrm{surf}}, \tag{6}$$

where σ_{el} represents conduction by dissolved ions in the pore fluids through interconnected pores. In addition, σ_w denotes the conductivity of the pore-filling electrolyte (conducting phase), and F is the formation factor, which depends on porosity ϕ and cementation exponent m (Archie, 1942) as $F = \phi^{-m}$, thereby reflecting both the volume and connectivity of the conducting phase. Furthermore, the additional conductivity σ_{surf} was initially attributed to "conductive solids" (Patnode & Wyllie, 1950), a term likely referring to clay minerals and their associated surface conduction. Winsauer and McCardell (1953) later recognized that this conduction arises from ion transport within the electrical double layer (EDL) at the mineral-fluid interface.

In addition to conduction, reversible charge storage occurs within the EDL at mineral-fluid interfaces. Accordingly, surface polarization can be incorporated into Equation 6 (Lesmes & Frye, 2001), which defines the complex conductivity (σ*):

$$\sigma^* = \sigma_{el} + \sigma_{\mathrm{surf}} = \frac{\sigma_w}{F} + \sigma'_{\mathrm{surf}} + i\sigma''_{\mathrm{surf}}, \tag{7}$$

where the real part of the surface conductivity (σ'_{surf}) represents charge conduction in the EDL and the imaginary part (σ''_{surf}) represents the reversible temporary charge storage. The real and imaginary parts of the measured complex conductivity (Equation 1) are related to the electrolytic and surface conductivity mechanisms as follows:

$$\sigma' = \sigma_{el} + \sigma'_{\mathrm{surf}}, \tag{8}$$

$$\sigma'' = \sigma''_{\mathrm{surf}}. \tag{9}$$

Equation 8 is consistent with Equation 6, where the measured conductivity represents the sum of conductivities arising from the parallel electrolytic and surface-conduction pathways within the porous medium. The real conductivity is governed by pore-fluid salinity, as the electrolytic component exhibits a linear dependence on fluid conductivity described by Archie's law (i.e., $\sigma_{el} = \sigma_w/F$). Surface conductivity σ'_{surf} contributes to the overall real conductivity, particularly under lower salinity conditions, but becomes less influential at higher salinities. In addition, the imaginary conductivity is governed by surface polarization and electrolytic conduction;

however, its salinity dependence is considerably weaker than that of the real conductivity. While some models attribute the salinity dependence of σ'' to variations in EDL properties (e.g., Revil & Skold, 2011), others emphasize the role of geometric and coupling effects between the EDL and the electrolytic phase (e.g., Qi & Wu, 2024).

The normalized chargeability M_n, first introduced by Keller (1959) for time-domain IP and later adopted in spectral IP by Lesmes and Frye (2001), is defined as

$$M_n = \sigma_\infty - \sigma_0 = M \cdot \sigma_\infty. \tag{10}$$

Slater and Lesmes (2002) showed that M_n can serve as a reliable proxy for clay content alongside σ'', implying the existence of ratios between σ'_{surf}, σ'', and M_n. This relationship was later formalized by Weller et al. (2013), who introduced the ratio $l_{mn} = M_n / \sigma_{\text{surf}}$ ($l_{mn} \approx 0.2$).

We assume that conductivity does not vary strongly with frequency, which is the case for porous rocks (Vinegar & Waxman, 1984) and soils. Under the constant phase angle assumption, the imaginary conductivity is determined near the peak frequency, taken as the geometric mean of a low frequency at which conductivity approaches σ_0 and a high frequency at which it approaches σ_∞. In this case, the relationship between M_n and σ'' can be written as

$$M_n \approx -\left(\frac{2}{\pi} \cdot \ln D\right)\sigma''. \tag{11}$$

where D denotes the number of decades separating high and low frequencies.

In media containing conductive solids, charge transport occurs within the mineral in addition to through electrolytic pathways within the pore space (Revil et al., 2015). Charges within the electron conductor are polarized with a resulting redistribution of ionic counter charges in the surrounding electrical double layer and electrolyte. Metal-electrolyte interfaces act as barriers that impede the movement of ions in the electrolyte and electrons in the minerals (Marshall & Madden, 1959; Sumner, 1976). Therefore, IP is particularly effective for characterizing subsurface properties and processes related to electron-conducting particles (e.g., ZVI), owing to the pronounced polarization enhancement typically exhibited by these particles. Both the volume concentration and size properties of such particles are potentially extractable.

The electrical properties of porous media are related to the material types (with or without conductive particles), pore network geometry (porosity, connectivity, surface area), properties of the contaminant (type, concentration, history, degradation) and the pore-filling fluids (relative concentrations, distributions and temperature). During in situ remediation, the correlation between geophysical responses and monitoring parameters (e.g., hydrochemistry, temperature, contaminant indicators) is critical for utilizing these data to evaluate remediation effectiveness. In this review, geophysical parameters are categorized into three types based on their physical and chemical properties during in situ remediation: conduction, polarization, and relaxation time (Table 1).

Specifically, this review focuses on the variation in electrical conductivity (or resistivity) as a key electrical property for characterizing remediation processes. For example, during ISCO remediation, the injection of chemical reagents into the contaminated medium results in highly conductive porous fluids due to elevated ion concentrations. Similarly, increased temperature enhances pore fluid conductivity by increasing the mobility of ions during ISTR.

Polarization properties refer to the charge storage behavior of subsurface media. Key parameters include chargeability, phase, normalized chargeability, and imaginary conductivity. Note that, although chargeability or phase are not a unique measure of polarization, since they are proportional to the polarization strength of the medium divided by the electromigration strength of the medium (Equations 3 and 10), we have classified them among the parameters representing polarization properties. This property arises from two distinct polarization mechanisms: (a) polarization of the EDL at the solid-liquid interface of insulating soil grains, and (b) polarization of the charges in the electron-conducting mineral grains (e.g., ZVI) and the balancing charge redistribution in the EDL and electrolyte around the grain. During remediation, measurable IP responses are driven by dynamic changes at polarizable interfaces, including electrochemical processes (e.g., sorption, ion exchange), mineral precipitation (conducting and/or insulating), and associated morphological and compositional transformations. The relaxation

Table 1
Electrical Properties Characterized by Electrical Geophysical Methods (Modified From Binley et al., 2015)

Electrical geophysical method	Electrical properties	Measured parameters	Examples of derived properties	
			Primary controls	Secondary controls
ERT	Conduction properties	Resistivity/conductivity	Pore fluid conductivity, temperature, types and geometrical arrangements of contaminants, etc.	Moisture content, porosity, surface area, clay content, etc.
TDIP	Conduction properties	Resistivity/conductivity, real conductivity, etc.	Clay content, surface area, geochemical transformations, surface electrochemistry, types and geometrical arrangements of contaminants, etc.	Pore fluid composition, moisture content, temperature, porosity, permeability, etc.
	Polarization properties	Chargeability, imaginary conductivity, phase, normalized chargeability, etc.		
	Relaxation time	Relaxation time, scaled relaxation time, etc.		
SIP	As above but with frequency dependence			

time correlates with characteristic length scales of polarization processes that are often related to the particle size distribution or pore size distribution. For contaminant removal processes that alter remediation material size through steps like adsorption, reduction, and co-precipitation (e.g., ZVI or AC in PRBs), polarization magnitude and relaxation time are effective parameters for characterizing the volume and relative size changes of polarizable materials, respectively (e.g., Niu & Revil, 2016; Pelton et al., 1978).

3. Concerns Regarding the Monitoring of In Situ Remediation Processes

In the following sections, we first introduce the principles, strategies, and applicable contaminant types of various in situ remediation techniques. Then, we present the monitoring parameters that should be considered based on the specific remediation process. Finally, we provide case studies that demonstrate the application of electrical geophysical methods for dynamic monitoring.

3.1. In Situ Chemical Remediation

ISCO/ISCR involves injecting oxidants or reductants into the subsurface to degrade toxic contaminants into less toxic or potentially non-toxic compounds (Figure 1a; Del Reino et al., 2014). Specifically, ISCO refers to the chemical reduction of contaminants at lower natural oxidant demand (NOD) condition, typically using permanganate (MnO_4^-), hydrogen peroxide (H_2O_2) and iron (Fe^{2+}) (Fenton reagent), and persulfate ($S_2o_8^{2-}$) (Zhang et al., 2017); whereas ISCR refers to the chemical reduction of contaminants at lower oxidation reduction potential (ORP) and dissolved oxygen (DO) conditions, typically using ZVI (Wu et al., 2024). ISCO technology is well-suited for treating a wide range of contaminants, including petroleum hydrocarbons, BTEX compounds (benzene, toluene, ethylbenzene, xylene), phenols, methyl tert-butyl ether (MTBE), chlorinated organic solvents, polycyclic aromatic hydrocarbons (PAHs), and pesticides (Huling & Pivetz, 2006). In contrast, ISCR technology is commonly used to remediate halogenated ethenes and ethanes, energetics, and some metals/metalloids (chromium (VI), arsenic, and uranium) (Cundy et al., 2008).

The effective delivery of oxidants or reductants to the target area is critical to the success of ISCO or ISCR, which is influenced by hydrogeological conditions, contaminant indicators, and reagent properties. Conversely, the injection of oxidants or reductants can also impact aquifer permeability, temperature, and the chemical and biological environments of the subsurface (Tratnyek et al., 2014; Wei et al., 2022; Table 2). Specifically, heterogeneity may influence the preferential pathways after oxidants or reductants injection, such that hydraulic gradients can be used to evaluate the hydraulic connectivity between injection and monitoring wells and potential migration pathways (Zehe et al., 2021). In contrast, the precipitation of oxidants (e.g., $KMnO_4$)/reductants (e.g., nanosized ZVI) may result in reduced permeability in or near the injection well (Kang et al., 2004; Phenrat et al., 2007). For example, manganese dioxide (MnO_2), the primary reaction byproduct following $KMnO_4$ injection, may accumulate near the injection wells or at the NAPL interface (i.e., encrustment), resulting in limited mass transport (reduced permeability) and decreased mass transfer efficiency. Additionally, contaminant type, phase, concentration and distribution determine the selection of remediation reagent and injection locations.

Table 2
Site Characterization Data Needed for in situ Remediation

	ISCO/ISCR	ISB	ISTR	PRB
References	Tratnyek et al. (2014), Wei et al. (2022)	EPA (2013), Romantschuk et al. (2023)	USACE (2014), Davis (2023)	ITRC (2011), Mak and Lo (2011)
Factors	Purpose of the information			
Hydrogeology	• Soil and aquifer parameters (e.g., stratigraphic heterogeneity, hydraulic conductivity and gradient): post-injection flow direction and rates	• Soil and aquifer parameters (e.g., stratigraphic heterogeneity, hydraulic conductivity and gradient): bioremediation coverage	• Soil and aquifer parameters (e.g., porosity, moisture content): adsorption and thermal desorption conditions	• Soil and aquifer parameters (e.g., stratigraphic type, groundwater level, hydraulic conductivity and gradient): PRB dimensions and location
Temperature	• Soil/groundwater temperature: activation condition	• Air/Soil/groundwater temperature: microbial activity	• Soil/groundwater temperature: heating coverage	• Soil/groundwater temperature: material reaction longevity
Hydrochemistry	• ORP/EC/DO/pH/microbiological indicator: injected reagent coverage; activation or redox condition; • Anions and cations (e.g., Fe (II), Mn (II), SO_4^{2-}): redox conditions	• ORP/EC/DO/pH/anions and cations (e.g., NO_3^-, SO_4^{2-}): microbial activity; • Microbiological indicator: bioremediation coverage	• ORP/EC/DO/pH/anions and cations: changes in groundwater quality	• ORP/EC/DO/pH/microbiological indicator/anions and cations (e.g., NO_3^-, SO_4^{2-}): material reaction longevity
Contaminant	• Contaminant type: remediation reagent type; • Distribution: injection well locations; • Phase/concentration: injection strategies and reagent mass	• Contaminant type/phase/concentration: microbiological type; • Distribution: injection well locations	• Contaminant type/phase/concentration: target temperature and heating type; • Distribution: heating and vapor extraction wells locations;	• Contaminant type/phase/concentration: material type; • Distribution: PRB dimensions and location

Moreover, the elements O, S, Mn and Fe are injected at high concentrations during ISCO/ISCR and serve as predominant participants in groundwater redox processes (Liu et al., 2022; Zhang et al., 2022). Secondary effects from the injection of these reagents encompass temperature variations, chemical alterations, and biological impacts driven by redox reactions and enhanced microbial activity. Therefore, temperature and hydrochemical parameters (e.g., ORP, DO, electrolyte conductivity (EC), pH, microbiological indicator, anions and cations) can be utilized to evaluate the activation and redox status of a remediation reagent and its range of impact.

An increasing number of studies have utilized electrical geophysical methods to delineate variations in the physical and chemical properties of contaminants during in situ chemical remediation (e.g., Ciampi et al., 2024; Flores Orozco et al., 2019; Hort et al., 2014; Mellage, Smeaton, et al., 2018). In the case of ISCO remediation process, Halihan et al. (2012) and Harte et al. (2012) employed ERT to characterize the degradation of hydrocarbon contamination and demonstrated that the observed reduction in resistivity was attributable to oxidant migration. Similarly, Bording et al. (2020) captured a high-conductivity anomaly, generated by the spreading of highly conductive oxidants, using cross-borehole resistivity. Moreover, subsequent experiments and field studies further quantified the contributions of contaminant degradation (5%–30%) and oxidant migration (70%–95%) to changes in electrical parameters during ISCO remediation (Harte et al., 2012; Xia, Ma, et al., 2023; Xia et al., 2025a).

Similar to oxidants, reductants also induce substantial changes in electrical parameters following injection. For example, Joyce et al. (2012) demonstrated that the polarization effect of porous media increases with higher concentrations of silver (Ag) or ZVI particles, whereas the polarization response of metal oxides is negligible. Moreover, electrical images during field-scale ISCR revealed an increase in polarization response (~20%) after ZVI injection, attributed to the accumulation of metallic surfaces at which the polarization takes place (Flores Orozco et al., 2015). Despite the significant changes in electrical images caused by the injection of oxidants or reductants, establishing quantitative correlations between electrical parameters and specific subsurface properties (e.g., temperature, hydrochemistry, contaminant concentration) is often challenging. Nevertheless, electrical geophysical methods may be highly valuable for determining the spatial distribution of subsurface changes, thereby guiding efficient direct sampling to accurately evaluate in situ chemical remediation processes.

3.2. In Situ Bioremediation

The process of in situ bioremediation (ISB) enhances the metabolism of target contaminants using indigenous bacterial communities. This is achieved by adding various amendments (biostimulation) to the subsurface environment or by introducing specific bacterial strains (bioaugmentation) to assist in treating contaminated sites (Figure 1b; Sturman et al., 1995; Vogt & Richnow, 2013). This technology has been effectively employed to decontaminate chlorinated solvents, dyes, nutrients, heavy metals, and organic waste sites (Sarkar et al., 2017).

The key to efficient in situ bioremediation is maintaining the biological activity that can degrade target contaminants. To accelerate bioremediation, the local conditions can be modified to promote robust microbial growth and metabolism, ensuring the effective degradation of the target contaminant or its components (Conrad et al., 2010). Environmental parameters, including temperature, hydrochemical parameters (e.g., ORP, pH), oxygen levels, and nutrient availability, should be optimized and adjusted according to hydrogeological conditions and contaminant indicators to support bacterial communities with the highest degradation potential (Table 2; EPA, 2013; Romantschuk et al., 2023). On the one hand, the type, phase, concentration, and spatial distribution of contaminants dictate the selection and location of injected amendments or bacterial strains. On the other hand, hydrogeological conditions, especially heterogeneity, hydraulic conductivity and gradient, govern the transport and distribution of these amendments or bacterial strains (Mahmoudi et al., 2020). Moreover, even if the bioremediation impact area fully encompasses the target contaminated area, ISB may still be inhibited for several reasons: limited availability of electron acceptors, donors, or nutrients; absence of biodegrading microbes; temperature not optimal for degradation; and unfavorable pH values, salinity, or redox conditions (Majone et al., 2015). Consequently, temperature and hydrochemistry are key parameters to monitor during ISB processes.

Numerous studies have been published on geophysical monitoring of ISB processes at laboratory (e.g., Song et al., 2024; Zhang et al., 2014) and field scales (e.g., Johnson et al., 2015; Nivorlis et al., 2024). The dependence of complex conductivity on the presence of microorganisms was shown in flow-through reactor or column experiments performed with mixed cultures and different contaminant media (Mellage et al., 2018a, 2018b; Song et al., 2022), while experiments on microbially induced iron sulfide transformations demonstrated the sensitivity of IP signals to microbe-mineral interactions (Personna et al., 2008; Williams et al., 2005). Such studies demonstrate that the abundance and growth stage of bacteria not only influence the concentration and distribution of charged particles at the solid-liquid interface but also that the charged bacterial cells themselves directly generate IP effects. Geophysical monitoring results of field-scale ISB processes reveal that the electrical responses of the aquifer undergoing bioremediation exhibit significant changes (Chambers et al., 2010; Williams et al., 2009). These changes are attributed to contaminant transformation and the release of microbial metabolic products (Caterina et al., 2017). In summary, variations in electrical properties are predominantly governed by microbial activity, which is influenced by temperature, hydrogeological conditions, and chemical and biological environments (Atekwana & Atekwana, 2010). Additionally, high polarization anomalies observed in aquifers following long-term bioremediation are likely linked to the formation of dispersed iron sulfide minerals (Kessouri et al., 2022).

3.3. In Situ Thermal Remediation

ISTR technology relies on delivering heat to the subsurface to alter the phase distribution and other physical properties of contaminants, facilitating their mobilization and recovery (Figure 1c; Johnson, Dahlen, et al., 2009). According to the different heating methods, ISTR includes steam-based heating, conductive heating, electrical resistance heating, radio-frequency heating, and large-diameter auger mixing with steam injection (Ding et al., 2019; Ramirez et al., 1993, 1995). Specifically, ISTR technology is widely applied to the remediation of volatile organic compounds (VOCs) and semi-volatile organic compounds (SVOCs) in soil and groundwater, including chlorinated solvents, petroleum hydrocarbons, benzene homologs, polycyclic aromatic hydrocarbons (PAHs), organochlorine pesticides (OCPs), polychlorinated biphenyls (PCBs), and volatile inorganic contaminants like mercury (Horst et al., 2021).

The effectiveness of heat in removing contaminant mass depends on heat conduction, which is influenced by heat conductivity distribution and thermal gradients (Kingston et al., 2010). These are related to hydrogeological conditions, heating temperature, hydrochemical environment, and contaminant indicators (Colombano et al., 2020; Sun et al., 2024). As illustrated in Table 2, soil and groundwater properties, such as porosity, and moisture content, directly determine adsorption and thermal desorption conditions. In addition, temperature

variations indicate the heating coverage, whereas hydrochemical parameters (e.g., ORP, EC, DO, pH, anions and cations) reveal changes in groundwater quality. While contaminant type/phase/concentration governs target temperature and heating method selection, contaminant distribution dictates the placement of heating and vapor extraction wells (Davis, 2023; USACE, 2014). Understanding the dynamic changes of these factors during heating is essential for evaluating the progress and effectiveness of thermal remediation.

For in situ thermal remediation of contaminated sites, several studies have highlighted the effectiveness of electrical geophysical methods in delineating the subsurface dynamics during the heating process (e.g., Almpanis et al., 2023; LaBrecque et al., 1996; Ramirez et al., 1993; Xia, Zhang, et al., 2023). The experimental study by Iravani et al. (2020) revealed that, when the temperature increased from 20°C to 50°C, the resistivity of a sample consisting of glass beads saturated with 80% coal tar and 20% ultra-pure water decreased from approximately 115 Ω·m to 50 Ω·m. Similarly, field-scale ISTR results show that resistivity changes are closely associated with phase transitions in contaminants induced by increasing temperature (Trento et al., 2021). In addition to contaminant concentration and phase state, Iravani et al. (2022) found that saturation change has the primary role in resistivity and phase angle variations compared to temperature (5%–7%) during heating. Furthermore, Xia et al. (2025b) identified a slow decreasing trend in ORP and DO along with a decrease in resistivity with temperature rise. Accordingly, changes in temperature, moisture content, and hydrochemical environment during the remediation process may influence the type of multiphase interfaces and pore space geometry within the medium, which can alter conduction and polarization in the subsurface. Identifying the effects of several factors on electrical properties is vital for accurately tracking the progress of thermal remediation efforts.

3.4. Permeable Reactive Barriers

A PRB is an artificially created permeable zone that contains or creates a reactive treatment area designed to intercept and remediate a contaminant plume (Figure 1d; Mosmeri et al., 2018). The treatment zone may be created directly using reactive materials (e.g., AC and ZVI) or materials designed to stimulate secondary processes (e.g., adding carbon substrate and nutrients to enhance microbial activity) (Singh et al., 2023). The PRB technology is predominantly used to remediate heavy metals, radioactive isotopes, chlorinated aliphatic hydrocarbons, and several organic and inorganic contaminants (Sakr et al., 2023), as well as to promote denitrification (e.g., Gibert et al., 2008).

The effectiveness of the barrier is determined by its interaction with contaminants and its reactive material. Specifically, the size and hydraulic properties of the barrier must be adequately designed to fully encompass the contaminated area while maintaining unobstructed groundwater flow. Additionally, the longevity of the PRB material's reactivity should guarantee the complete removal of contaminants (Budania & Dangayach, 2023; Gavaskar et al., 2002). Accordingly, the key indicators for evaluating PRB performance and longevity comprise target contaminants and their degradation products, groundwater seepage properties within and around the PRB, temperature, and hydrochemistry (Table 2; ITRC, 2011; Mak & Lo, 2011). Specifically, the type, phase, and concentration of contaminant dictate the choice of PRB filling material. The length and depth of the PRB are determined by stratum properties and contaminant distribution, while the thickness is designed based on the required residence time of the contaminant and the groundwater flow velocity (Chen et al., 2016). The spatial and temporal hydraulic properties also influence the chemical environment of the aquifer and the PRB (Elder & Benson, 2018), thus the hydrochemical parameters (e.g., ORP, EC, DO, pH, anions and cations) are effective indicators for monitoring the long-term performance of PRB. Moreover, if the PRB performance enhances natural attenuation processes on the downgradient side, monitoring the temperature and microbiological indicators of the downgradient aquifer may be critical (Chen et al., 2018).

Previous laboratory and field studies have highlighted the potential of electrical geophysical methods for assessing barrier integrity and long-term performance of barrier materials (e.g., Hao, Cao, et al., 2021; Slater & Binley, 2006; Wu et al., 2008). Slater and Binley (2003) validated the capability of 2D resistivity imaging and cross-borehole IP to characterize ZVI integrity variations within a ZVI PRB. In addition, electrical geophysical methods have been explored for monitoring biological PRBs (Davis et al., 2010; Doherty et al., 2010). For example, Sentenac et al. (2015) utilized time-lapse ERT to monitor the remediation process of a biological PRB for diesel plume and observed the redistribution of diesel within the soil matrix. Moreover, secondary biogeochemical processes (e.g., mineral precipitation, gas accumulation) may influence barrier performance, potentially affecting electrical properties. For example, laboratory ZVI columns exhibited a notable increase in both the real

and imaginary parts of complex conductivity after the precipitation of iron hydroxides and iron carbonates (Hao, Ye, et al., 2021; Slater et al., 2005; Wu et al., 2005, 2006), while the precipitation of calcium carbonate inhibited the conductivity and polarization (Wu et al., 2009). Several studies have assessed the performance and remediation capabilities of geophysical methods in monitoring other reactive materials (e.g., AC and zeolite) (Bate et al., 2022; Moshe & Furman, 2022; Yang et al., 2024), particularly the combined remediation processes involving two or more different materials. For example, the removal efficiency of Cr(VI) is significantly enhanced when ZVI and AC are used in combination (Ma, Zhang, et al., 2025). Moreover, chargeability and relaxation time for combined ZVI and AC were found to be 2.4–4.3 times and 6.1–9.9 times that of using ZVI or AC alone respectively (Ma, Schwartz, et al., 2025).

These additional parameters provided by the IP method enhance our ability to evaluate changes in the electrochemical properties of materials within the PRB. Specifically, the polarization response exhibited by reactive materials such as ZVI and AC is markedly higher than that of non-conductive media like sand and clay. This phenomenon is attributed to the polarization of charge within the conductive mineral particles (i.e., electron conductors). Furthermore, physicochemical alterations in particle structure and composition from chemical reactions or adsorption can modify polarization amplitude and response time (Wu et al., 2008). Accordingly, IP measurements directly reflect the chemical reactions occurring within barriers, enabling comprehensive evaluation of reactive performance and hydraulic conductivity (Hao, Cao, et al., 2021).

3.5. Combined Remediation

Combined remediation integrates two or more distinct physical, chemical, or biological remediation technologies. Combining these diverse technologies not only addresses the limitations associated with using a single technology but also leverages the strengths of each method to enhance remediation efficiency significantly (Nie et al., 2024). Correspondingly, the integration of multiple in situ remediation technologies induces more complex alterations in subsurface physical, chemical, or biological conditions than single remediation technologies (Ismail et al., 2023; Ma et al., 2017), presumably resulting in more complex variations in electrical properties during the remediation process.

An example of combined remediation is the joint use of remediation reagents or materials and bioremediation. Specifically, oxidants or reductants can affect the chemical environment (e.g., ORP, DO, pH, etc.) in the subsurface, thereby altering the growth conditions of microorganisms (Jia et al., 2025). As a material widely employed in ISCR and PRB, ZVI reacts with contaminants to establish anoxic conditions, elevate H_2 concentration and pH, and facilitate the formation of Fe(II)/Fe(III) compounds (Shi et al., 2015; Wu et al., 2020). This creates a favorable microenvironment for microorganisms, thus promoting long-term bioremediation. Lévy et al. (2022) and Thalund-Hansen et al. (2023) utilized cross-hole ERT and IP to monitor reagent diffusion and biodegradation processes following ZVI injection. The geophysical data were then used to provide estimates of the distribution of hydraulic conductivity (K) and contaminant mass discharge.

Another example is the combination of in situ thermal and ISCO or bioremediation. Heating not only alters the physical and chemical state of contaminants but also acts as an activation condition for oxidants and enhances the activity of bacterial communities (Wang et al., 2017, 2022). Given this complexity, monitoring the spatiotemporal evolution of these coupled processes is critical. Xia et al. (2025b) employed the time domain IP (TDIP) method alongside hydrogeological parameters and contaminant measurements to monitor the in situ thermal-enhanced oxidative remediation process at a NAPL-contaminated site, quantify contaminant removal during heating, and determine the migration path of the injected oxidant. They found that changes in IP parameters were directly related to temperature, hydrochemistry, groundwater level, oxidant migration, and NAPL removal. In addition, Tsakirmpaloglou et al. (2020) utilized IP to monitor the biodegradation process of hydrocarbons by indigenous bacteria and/or fungi under in situ heating conditions. The IP results indicate that high chargeability anomalies were predominantly concentrated near the groundwater level, where contaminant concentrations and oxygen availability were higher compared to other areas.

3.6. Workflow Implementation of Electrical Geophysical Methods for in Situ Remediation

To achieve optimal monitoring resolution, geophysical deployment strategies must be customized according to specific in situ remediation technologies. This review focuses specifically on electrode configuration strategies for ERT and IP methods, with deployment details primarily derived from synthesis of existing literature. As

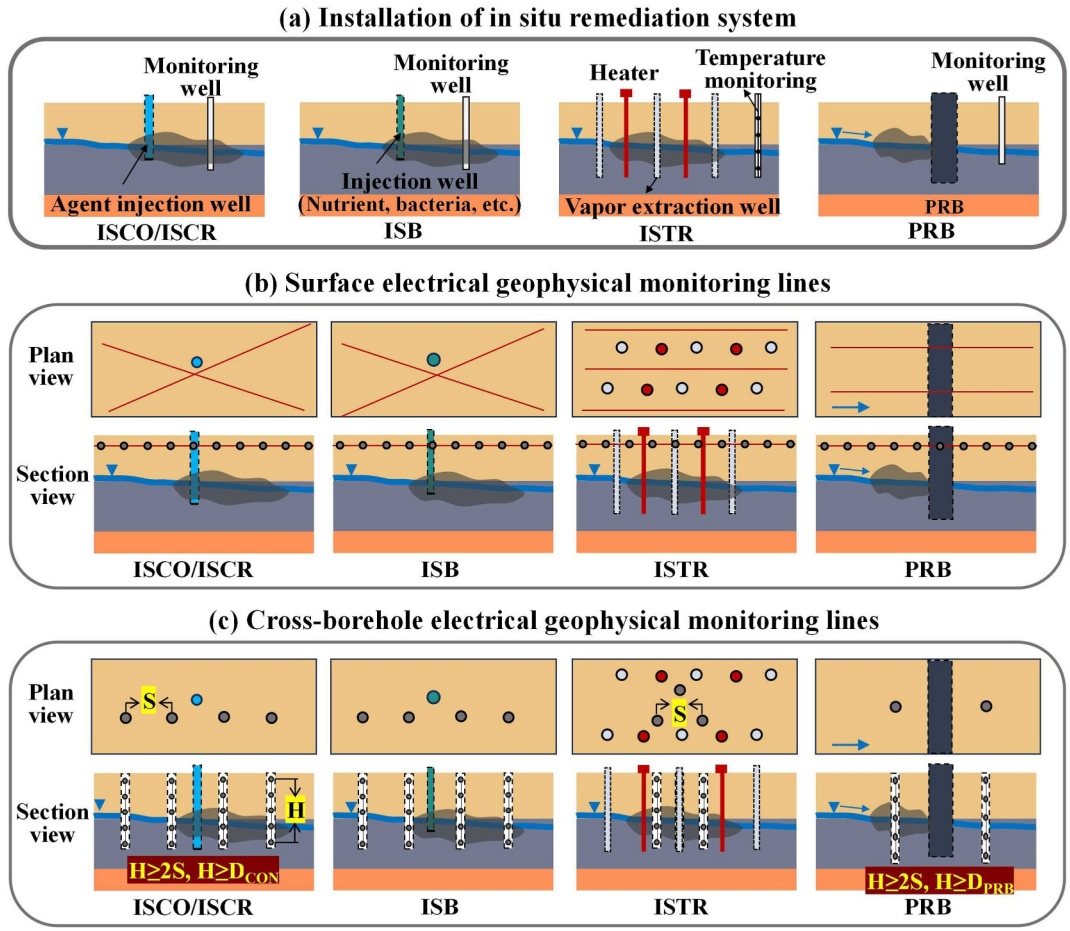

Figure 4. The general workflow for application of electrical geophysical methods. Both ERT and IP methods can be deployed using either surface or cross-borehole electrode configurations, deployment strategies must be customized according to specific in situ remediation technologies and site conditions.

shown in Figure 4a, field deployment for in situ remediation requires customized configuration parameters based on contaminant indicators and site conditions, while geophysical monitoring cables are typically deployed only after a remediation system installation is complete. Ideally, monitoring should begin prior to remediation to establish a reliable baseline, as tracking changes relative to this initial state enhances the usefulness of geophysical data. Furthermore, the selection of configurations and measurement options, such as surface or cross-borehole, should be optimized based on field conditions and expected signal quality. Surface configurations offer broad areal coverage with minimal disturbance to the strata, while cross-borehole setups provide higher resolution for targeted areas between boreholes (Binley & Slater, 2020). Measurements are typically taken using stainless steel electrodes; however, non-polarized electrodes (e.g., Cu-$CuSO_4$ and Pb-$PbCl_2$) are occasionally employed in IP surveys to eliminate electrode polarization effects (Petiau, 2000). Furthermore, separating current and potential circuits with distinct multi-conductor cable spreads can decrease capacitive coupling and enhance geophysical data quality (Dahlin & Leroux, 2012). For example, by combining stainless steel and non-polarized Pb-$PbCl_2$ electrodes with cable arrangements designed to reduce capacitive coupling, Xia et al. (2025b) achieved an improved signal-to-noise ratio in their IP monitoring of in situ thermal-enhanced oxidative remediation.

The typical design and deployment of surface monitoring lines are illustrated in Figure 4b. While maintaining straight survey lines, the depth of investigation should encompass the entire remediation zone. In general, the depth of investigation increases with electrode array spacing and total array length, but it also depends on array configuration and on the conductivity structure of the subsurface. Additionally, signal strength and site-specific noise levels also affect the depth at which data can be reliably distinguished (e.g., Binley & Slater, 2020; Edwards, 1977). However, the optimization of array protocol may reduce the required line length. For example,

Flores Orozco et al. (2015) monitored the ISCR process using TDIP through a Dipole−Dipole array that combines measurements with dipole lengths of 4, 5, and 6 m, respectively. They employed a 23 m survey line to investigate the ZVI injection at a depth of 10.5 m. In addition, for PRB remediation sites, the surface survey lines should be arranged to extend across the barrier. Ideally, the line length should be at least five times the barrier's buried depth. Slater and Binley (2003) demonstrated an alternative deployment, in which they conducted a 2D surface imaging survey along the long -axis of the barrier to constrain the lateral extent of the barrier along its axis.

The design and deployment of the cross-borehole configuration are shown in Figure 4c. In particular, the depth of the deepest electrode should be set to exceed both twice the borehole spacing and the stratigraphic depth of the contaminant plume. The plan view of geophysical monitoring boreholes may follow a linear arrangement (e.g., ISCO/ISCR and ISB in Figure 4c) or alternative configurations such as a triangular arrangement (e.g., ISCR in Figure 4c). For example, Bording et al. (2020) employed collinear dipole-dipole single borehole measurements, parallel cross-borehole dipole-dipole arrays, and equatorial cross-borehole dipole-dipole arrays to monitor ISCO remediation through cross-hole TDIP measurements. In addition, when implementing cross-borehole monitoring at PRB remediation sites, the borehole depths should be designed to exceed the burial depth of the barrier (e.g., Slater & Binley, 2003, 2006).

4. Factors Affecting Electrical Properties During In Situ Remediation

Growing evidence demonstrates the applicability of geophysical methods for real-time monitoring of in situ remediation processes. The remediation process drives complex alterations in subsurface hydrogeological properties, temperature, hydrochemistry, and contaminant phase, distribution, and concentration. These changes can influence the types of multiphase interfaces and the geometry of pore spaces within the medium, consequently altering the conductive and capacitive of subsurface. As illustrated in Figure 3, monitoring parameters commonly mentioned in the literature are summarized based on their frequency of occurrence. Beyond electrical properties, key monitoring parameters include contaminant concentrations, stratum information, groundwater temperature, ionic composition (anions and cations), pH, etc. Accordingly, based on this analysis, we categorize monitoring parameters into four factors: hydrogeology, temperature, hydrochemistry, and contaminant indicators. In the following sections, we analyze representative studies and summarize the effects of hydrogeological conditions, temperature variations, hydrochemical parameter changes and contaminant removal on electrical parameters during in situ remediation.

4.1. Hydrogeology

Among hydrogeological parameters, hydraulic conductivity is of paramount importance, as it governs fluid flow and contaminant transport (Eggleston & Rojstaczer, 1998; Michael & Khan, 2016). These hydraulic properties can directly affect the spatial distribution of electrical parameters and must be characterized for effective remediation monitoring.

Hydrogeological heterogeneity can substantially complicate the delivery of remediation reagents or materials to contaminated zones and their subsequent interaction with target contaminants. Such heterogeneity is often present in NAPL-contaminated sites (Figure 5a), where contrasting lithologies and variable permeability create preferential flow paths that hinder effective reagent distribution (Zhang et al., 2019). Electrical geophysical methods are powerful tools for characterizing the hydrogeological properties of the strata. Johnson, Versteeg, et al. (2009) significantly improved the spatial resolution of hydraulic conductivity by supplementing sparse hydrogeological data with time-lapse resistivity data. Their findings highlighted the utility of incorporating multi-source data to estimate hydrogeological properties through the integration of electrical and hydrological information. Similarly, Thalund-Hansen et al. (2023) utilized cross-borehole IP to infer high resolution hydraulic conductivity (K) fields after injecting reagents containing ZVI, enabling NAPL contaminant mass discharge (CMD) estimation (Figure 5b). They emphasized that, compared to traditional monitoring wells, cross-borehole geophysical methods for estimating K-distribution significantly improve CMD-based evaluation of in situ remediation performance at contaminated sites. Specifically, IP offers distinct advantages over conventional resistivity methods for permeability estimation in unconsolidated sediments (Weller et al., 2015). While direct current resistivity methods are primarily sensitive to bulk conductivity, IP measures surface polarization effects that are directly linked to pore geometry, including the specific surface area per pore volume, a key length scale controlling permeability in granular media (Weller et al., 2010).

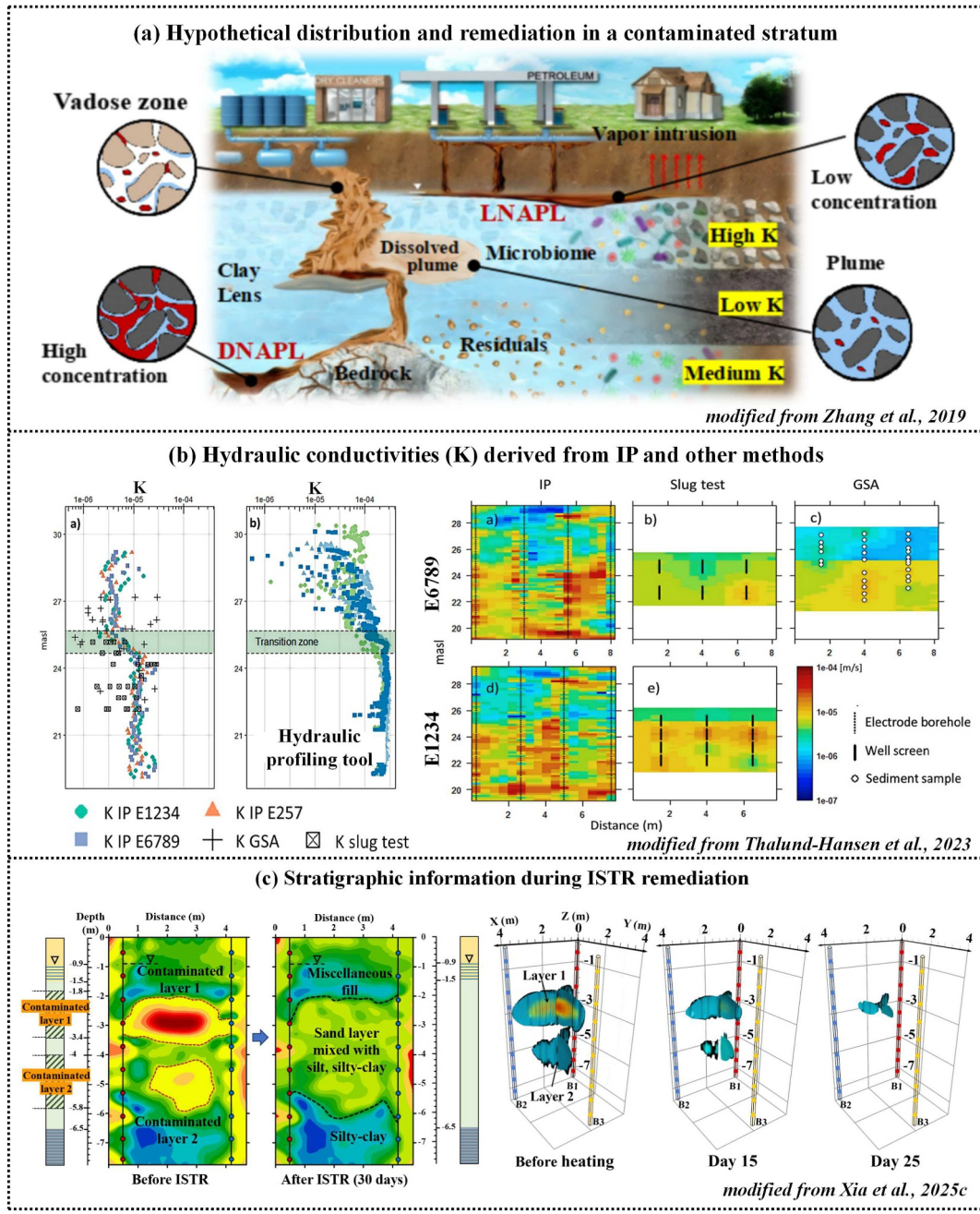

Figure 5. Influences of hydrogeology on electrical parameters during remediation. Hydrogeological heterogeneity influences contaminant distribution and remediation efficiency (Zhang et al., 2019). Accordingly, it determines the baseline of electrical parameters (Thalund-Hansen et al., 2023), while remediation alters these conditions, thereby inducing corresponding shifts in geophysical properties (e.g., Xia et al., 2025c).

Moreover, changes in stratigraphic features during in situ remediation can significantly influence the electrical responses measured by electrical geophysical methods (Table 3). In one study, ISCO/ISCR induced a 68.2% increase in bulk electrical conductivity of sand with <2% silt/clay content through oxidant/reductant injection and contaminant degradation (Harte et al., 2012). Additionally, Sparrenbom et al. (2017) utilized TDIP to monitor the ISB remediation process and discovered that bedrock surface subsidence facilitated microbial degradation of contaminants, whereas a fracture zone contributed to the loss of remediation reagents. Similarly, Xia et al. (2025c) monitored the ISTR remediation process using cross-hole ERT integrated with drilling sampling (Figure 5c). The

Table 3
Hydrogeological Features and Related Key Electrical Properties for Different Site Remediation Technologies

Technology	Hydrogeology features	Contaminant	Key electrical parameters	Methods	References
ISCO/ ISCR	Medium to coarse sand with <2% silt/clay	Tetrachloroethene (PCE)	Conductivity of 8.7 mS/m before remediation; Conductivity increases to 27.3 mS/m after permanganate injection	ERT	Harte et al. (2012)
ISB	Sediments, high quality and low quality rock	Trichlorethylene (TCE) and metabolites	Subsidence of the bedrock surface leads to the accumulation of contaminants and carbon sources, enabling microbial degradation and resulting in a chargeability difference > 5 mV/V	TDIP	Sparrenbom et al. (2017)
ISTR	Sand layer mixed with silt and silty-clay	Chlorobenzene and PCE	Resistivity of strata with contaminants 55–320 Ω·m before heating; Average resistivity decreases to 35 Ω·m after heating	Cross-borehole ERT	Xia et al. (2025c)
PRB	Sand, silt, and basal gravel	Vinyl chloride (VC) and cis-DCE	About 3 years after PRB installation, the conductivity of the sand, silt, and basal gravel is 0.04 S/m, whereas the conductivity of PRB filled with reactive iron is 10^5 S/m	ERT, SIP, Cross-borehole ERT	Slater and Binley (2003, 2006)

resistivity distribution revealed stratigraphic changes following heating, that is, the average resistivity of the contaminated zone decreased by 45%–89%. In contrast, Slater and Binley (2003) observed that, approximately 3 years after installation, the conductivity of a PRB filled with active iron was 10^5 S/m: significantly higher than that of sand, silt, and basal gravel. This conductivity contrast, attributed to the electronic conductor (ZVI), was deliberately exploited to verify the effective emplacement of PRB (Slater et al., 2005). In general, pre-remediation hydrogeological heterogeneity governs the baseline distribution of electrical parameters, while subsequent in situ remediation dynamically alters subsurface conditions, inducing corresponding shifts in geophysical responses.

4.2. Temperature

Temperature variations during remediation directly affect the electrical responses of subsurface media through saturation changes, promotion of fluid viscosity, ion mobility, contaminant removal, microbial activity and growth.

For thermal remediation of NAPL-contaminated media, Xu et al. (2024) demonstrated that remediation effectiveness hinges on co-boiling at the water-NAPL interface (Figure 6a), highlighting the need to capture spatiotemporal temperature evolution. Several studies have demonstrated that temperature variations during heating can significantly affect the electrical parameters. For example, Iravani et al. (2022) employed SIP to quantify the effects of temperature changes and fluid saturation changes, caused by water displacement of coal tar, on measured complex resistivity (Figure 6b). Their findings revealed that the influence of saturation changes on complex resistivity phase angle was considerably more significant than that of temperature. Similarly, as illustrated in Table 4 for ISTR, resistivity decreases with rising temperature until the fluid's boiling point, and increases as temperature rises further due to decreased saturations and generation of gases (Iravani et al., 2020, 2022; Trento et al., 2021), indicating that resistivity interpretation can be ambiguous when both fluid saturation and temperature change concurrently. Xia et al. (2025c) used cross-borehole ERT to quantitatively analyze the effects of contaminants and temperature on subsurface resistivity at the field scale. Based on the relationship between resistivity and temperature, the spatiotemporal distribution of effective energy consumption for contaminant removal was delineated by tracking resistivity variations (Figure 6c).

Beyond thermal remediation, temperature serves as a critical parameter influencing geophysical monitoring signals across other in situ remediation techniques (Table 4). Specifically, for in situ thermal-enhanced oxidative remediation, the combined effects of temperature increase and thermally activated persulfate injection result in pollutant removal and enhanced ion mobility, leading to a significant decrease in resistivity and chargeability within the vertical heating zone (Xia et al., 2025b). Caterina et al. (2017) hypothesized that in the ISB process, a 1° C rise in temperature during bioremediation leads to a 2% increase in bulk conductivity, which was applied to assess the impact of seasonal temperature shifts on bacterial activity and growth, given that higher temperature

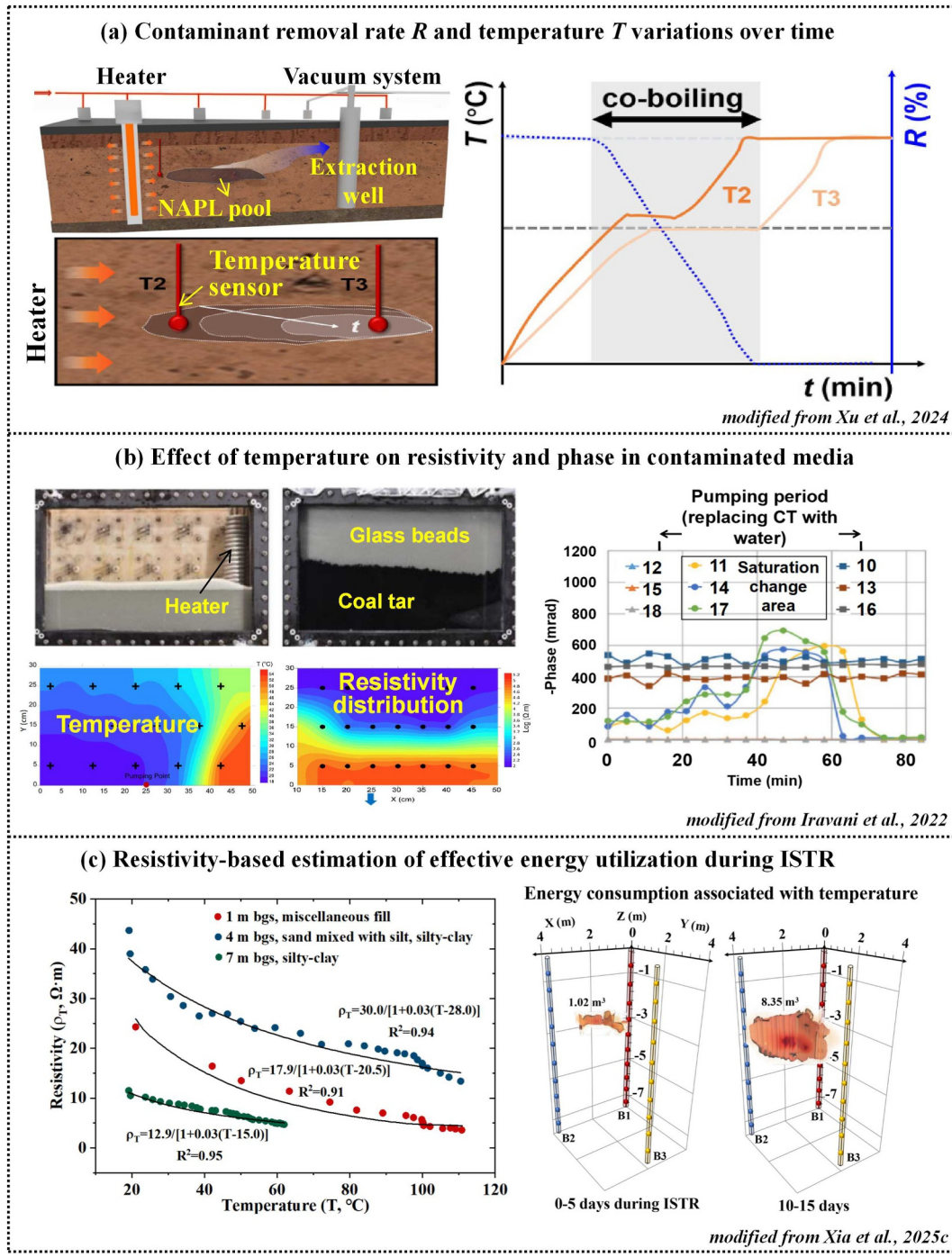

Figure 6. Influences of temperature on electrical parameters during remediation. Accurately capturing the spatiotemporal changes in temperature is crucial for both evaluating contaminant removal and optimizing energy consumption (Xu et al., 2024). Electrical geophysical methods offer an effective approach by utilizing electrical parameters to characterize contaminant removal process with temperature (Iravani et al., 2022), and guide strategies to reduce energy waste (Xia et al., 2025c).

generally results in a higher enzymatic activity. Similar electrical responses may be found in biological PRB remediation processes. The increased conductivity with temperature is primarily attributed to enhanced fluid viscosity, ion mobility, and stimulated microbial activity and growth. In contrast, for PRBs filled with

Water Resources Research

10.1029/2025WR043172

Table 4
Examples of Temperature Effects on Electrical Parameters During Remediation Processes

Technology	Temperature change	Contaminant	Key electrical parameters	Temperature influence	Methods	References
ISCO/ ISCR	Soil and groundwater: >35°C	Benzo(a)pyrene (B[a]P), dibenz (a,h) anthracene (DBA)	Increased temperature and injected thermally activated persulfate are the main causes of IP changes during ISCO remediation	Activation reactions of remediation reagent, ion mobility	TDIP	Xia et al. (2025b)
ISB	Air: 20°C Soil: ~12°C Groundwater: 14°C	Hydrocarbon (C_{10}-C_{40})	Bulk conductivity increases by 2% for every 1°C rise in soil and groundwater temperature during bioremediation	Fluid viscosity, ion mobility, microbial activity and growth	ERT	Caterina et al. (2017)
ISTR	Soil and groundwater: >100°C	Coal tar	The resistivity decreases with rising temperature until the boiling point, and increases as temperature rises further beyond it	Combustion gas generation, air displacement of fluids, and contaminant removal	ERT	Iravani et al. (2020, 2022); Trento et al. (2021)
PRB	Seasonal variations	VC and cis-DCE	Changes in IP response may result from variations in an environment outside the barrier, for example, temperature, salinity, water content	Material reaction rate, reaction fronts at the barrier interface. Nevertheless, temperature effects are not considered a primary factor in the discussion of PRBs	SIP	Slater and Binley (2006); ITRC, (2011)

non-biological remediation materials such as ZVI, temperature changes may influence geophysical signals by altering the material reaction rate and reaction fronts at the barrier interface (ITRC, 2011).

4.3. Hydrochemistry

Understanding the relationship between hydrochemical and electrical parameters is essential for effectively evaluating, controlling, and optimizing in situ remediation processes. As exemplified by the ISCO-ISB process (Figure 7a), oxidant injection alters subsurface chemistry (e.g., pH, ORP, DO, EC), and the resulting bioavailable by-products subsequently enhance indigenous microbial activity (Honetschlägerová et al., 2019). Using electrical geophysical methods to map subsurface electrical properties provides valuable proxy indicators for inferring spatial and temporal changes within the treatment zone, although hydrochemical parameters may not be directly measured. This perspective is supported by several studies (e.g., Chen et al., 2013; Hort et al., 2015; Xia, Meng, et al., 2023). For example, Lévy et al. (2024) monitored in situ persulfate remediation at a large-scale site in Denmark using cross-borehole resistivity methods combined with chemical sampling. They established an empirical relationship between the monitored resistivity and the temporal evolution of sulfate concentrations in the system (Figure 7b), enabling quantitative interpretation of the geophysical data in terms of sulfate distribution (Table 5). Consequently, integrating electrical geophysics improves the predictive accuracy of transport models, rather than relying solely on pre-assumed hydraulic conductivity fields. Davis et al. (2006) conducted laboratory SIP measurements and combined them with hydrochemical analysis on soil undergoing biodegradation. They confirmed that measurable polarization results from the presence of biofilm itself in porous media, manifested as changes in the imaginary conductivity that are linked to variations in microbial cell concentration (Figure 7c). Similar conclusions were also found in the study by Nivorlis et al. (2024), that is, the correlation between geophysical imaging and hydrochemistry shows that chloride ions and iron ions generated during ISB are the main chemicals that can be correlated with resistivity (Table 5). These studies indicate that geophysics can serve as an alternative indicator of subsurface changes, but also suggest that anomalies require confirmation through direct hydrochemical sampling to identify specific contaminant transformation processes during remediation.

In addition to ISCO and ISB, hydrochemical analysis is essential for assessing the remediation performance of ISTR and PRB technologies. Almpanis et al. (2023) investigated the SIP properties during smoldering remediation supported by colloidal activated carbon. The results reveal that imaginary and real conductivity are sensitive to the smoldering process, relating to organic matter content and corresponding to the EC trend pre- and post-smoldering. Doherty et al. (2010) integrated geophysical monitoring with chemical and microbiological analyses to develop a conceptual biogeochemical model of the processes occurring around a contaminant plume during biological PRB remediation processes. These examples highlight the importance of geophysical monitoring in promptly identifying anomalies when significant subsurface changes occur. Such anomalies are crucial for triggering targeted direct sampling, which is essential for understanding the actual changes in aqueous geochemistry and contaminant transformations. This ability to guide the timing and location of critical sampling is a key advantage of geophysical methods in remediation monitoring.

4.4. Contaminant Indicators

Contaminant indicators, including type, concentration, distribution, and phase, directly assess remediation effectiveness and influence electrical parameters by altering pore-scale geometry and current paths. Moreover, contaminant transformation or degradation under changing physical, chemical, or biological conditions further complicates the electrical response.

Figure 8a illustrates the temporal behavior of bulk conductivity during biodegradation of hydrocarbons. Initially, fresh hydrocarbon spills decrease bulk conductivity because of their naturally resistive properties (stage A). As microbial degradation commences, the generation of organic and carbonic acids promotes mineral weathering, increasing pore-fluid electrolytic conductivity and thus bulk conductivity (stages B–C) (Atekwana et al., 2004a, 2004b; Naudet & Revil, 2005; Sauck, 2000). Eventually, as contaminants are removed, conductivity declines toward pre-spill levels (stage D) (Che-Alota et al., 2009).

Another example illustrating electrical signals in response to contaminant removal during synergistic ZVI/AC remediation applied in PRB is presented in Figure 8b, as highlighted by Ma, Zhang, et al. (2025). Chargeability and scaled relaxation time measured by SIP decrease simultaneously as Cr(VI) removal rates decline. Additionally, the correlation between chargeability and the active surface area can characterize the reactivity of

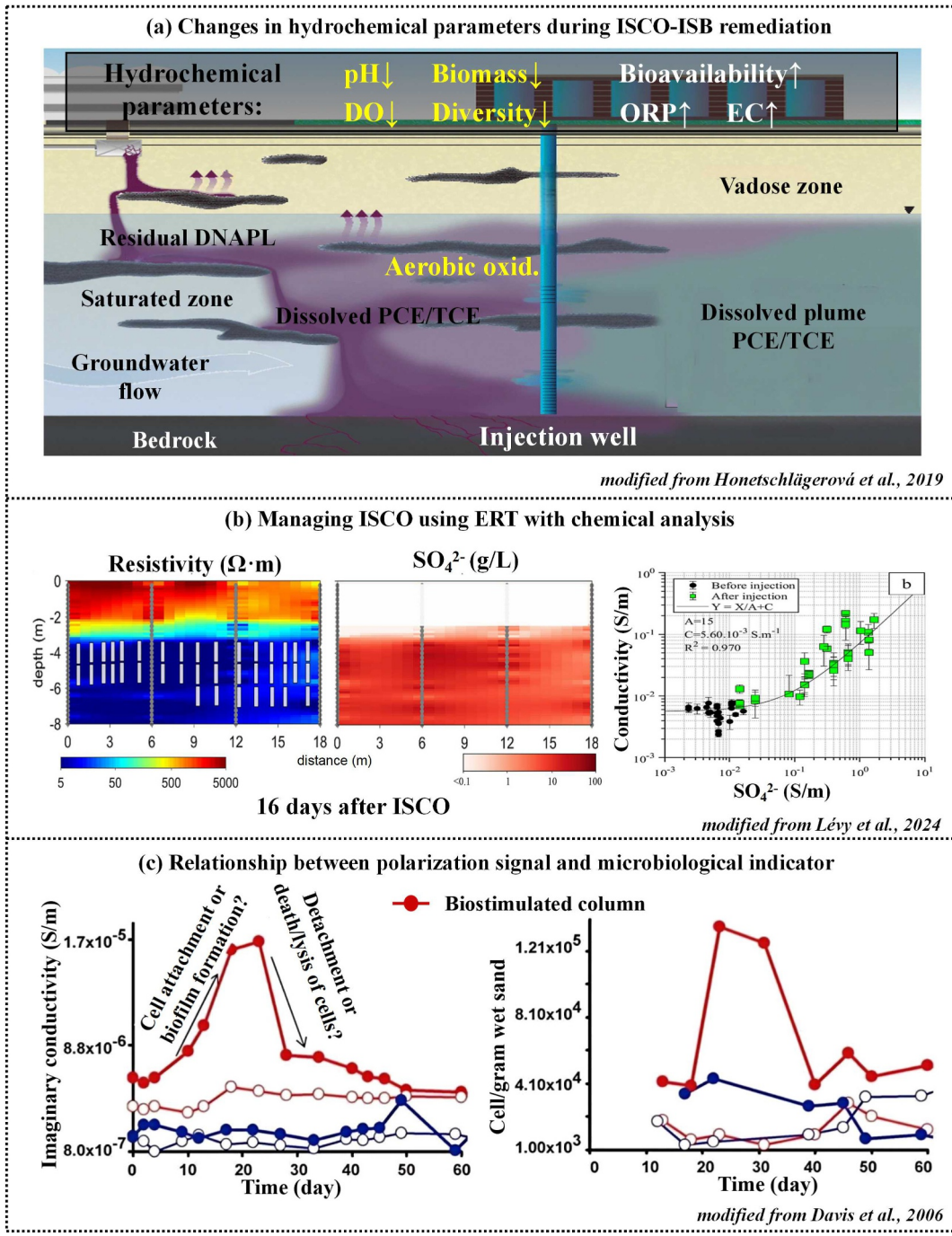

Figure 7. Influences of hydrochemistry on electrical parameters during remediation. Subsurface hydrochemical environments exhibit spatiotemporal dynamics during remediation processes (Honetschlägerová et al., 2019). As highlighted in previous studies (Davis et al., 2006; Lévy et al., 2024), establishing relationships between geophysical and hydrochemical parameters advances real-time characterization of biogeochemical conditions and the assessment of remediation effectiveness.

ZVI-AC particles. The scaled relaxation time exhibits a more pronounced dependence on variations in the radius of ZVI matrix. Specifically, the relaxation characteristic length decreases due to the reduction of the external low-polarization $(Cr_xFe_{1-x})(OH)_3$ shell and the internal ZVI matrix, resulting in a decreased scaled relaxation time.

Table 5
Examples of Hydrochemistry Effects on Electrical Parameters During Remediation

Technology	Hydrochemical parameters	Key electrical parameters	Methods	References
ISCO/ ISCR	EC, anions and cations (Cl^-, SO_4^{2-}, Ca^{2+}, and Na^+)	Resistivity is linearly related to salt concentration, that is, sulfate distribution converted from resistivity images represents effective reagent distribution and activation	Cross-borehole ERT	Lévy et al. (2024)
ISB	ORP, pH, anions and cations (e.g., Cl^-, SO_4^{2-}, $Fe^{2+/3+}$, Ca^{2+}, Mg^{2+}, Na^+)	Chloride ions and iron ions are the main chemicals that can be correlated with resistivity	TDIP	Nivorlis et al. (2024)
ISTR	EC, organic matter	Imaginary and real conductivity are sensitive to the smoldering process, relating to organic matter content and corresponding to the EC trend pre- and post-smoldering	SIP	Almpanis et al. (2023)
PRB	EC, pH, Anions and cations (e.g., NH^{4+}, SO_4^{2-}), enumeration of microorganisms, cloning 16S rRNA genes, sequencing	Normalized chargeability can reflect buried metals, clays, bioprecipitation, mineralization or accumulations of microbes present in the pore space and attached to the solid matrix	TDIP	Doherty et al. (2010)

Moreover, Xia et al. (2025a) monitored the ISCO remediation process of LNAPL using IP and proposed a new concept for the oxidation process of LNAPL in pores. The high-conductivity environment created by the injected oxidant with high ionic concentration suppresses the IP phenomenon. As the concentrations of ions such as SO_4^{2-}, HCO_3^-, and CO_3^{2-} increase during LNAPL degradation, the number of interfaces capable of polarization decreases, resulting in a decrease of chargeability response (Figure 8c). Consequently, this decline leads to the disappearance of the peak frequency and further decreases in phase and resistivity.

5. Toward Efficient in Situ Remediation Associated With Electrical Responses

As illustrated above, electrical geophysical methods serve as effective visualization tools to delineate the temporal dynamics of subsurface electrical responses during remediation, providing a robust approach for evaluating remediation efficacy. To further advance this capability, the integration with numerical modeling presents a promising approach for predicting contaminant degradation and transformation. A particularly powerful approach in this context is coupled hydrogeophysical modeling, which links hydrological and geophysical simulations to improve the interpretation of geophysical data in terms of hydrogeological and biogeochemical properties (Tso et al., 2020). For example, Almpanis et al. (2021) developed a DNAPL-DCIP model demonstrating the effectiveness of geophysical techniques in tracking DNAPL mass reduction, where resistivity delineated contamination zones and chargeability aided lithological interpretation (Figure 9a). Han et al. (2024) developed a real-time ISCO monitoring framework by integrating time-lapse ERT with reactive transport models (RTM), where bulk conductivity mapped ionic species distributions while model-derived data inferred dissolved TCE patterns (Figure 9b). Beyond fully coupled approaches, synthetic forward modeling alone can also provide valuable insights into the interpretability of geophysical monitoring. For example, Slater and Binley (2006) simulated the electrical evolution of a PRB over 30 years based on laboratory-derived conductivity changes expected due to barrier aging. Their results demonstrated that synthetic ERT and IP data could diagnose reactive front growth through barrier, even when the spatial resolution of front width was limited (Figure 9c). However, certain limitations remain regarding the independent interpretation of electrical parameters derived from laboratory and field measurements as well as numerical simulations. Therefore, calibration through direct borehole monitoring data is essential to ensure a reliable assessment of actual subsurface remediation processes.

Electrical geophysical methods serve as effective visualization tools that can support remediation management by capturing key process dynamics. These techniques serve as powerful visualization tools for (a) highlighting stratigraphic changes before and after remediation, (b) tracking real-time thermal, chemical, and biological variations, and (c) identifying contaminant transformation and degradation trends (Binley et al., 2015). However, as indirect proxies, these measurements may unable to independently quantify hydrological, thermal, hydrochemical, and contaminant variations. The interpretation of geophysical data is challenged by the non-uniqueness

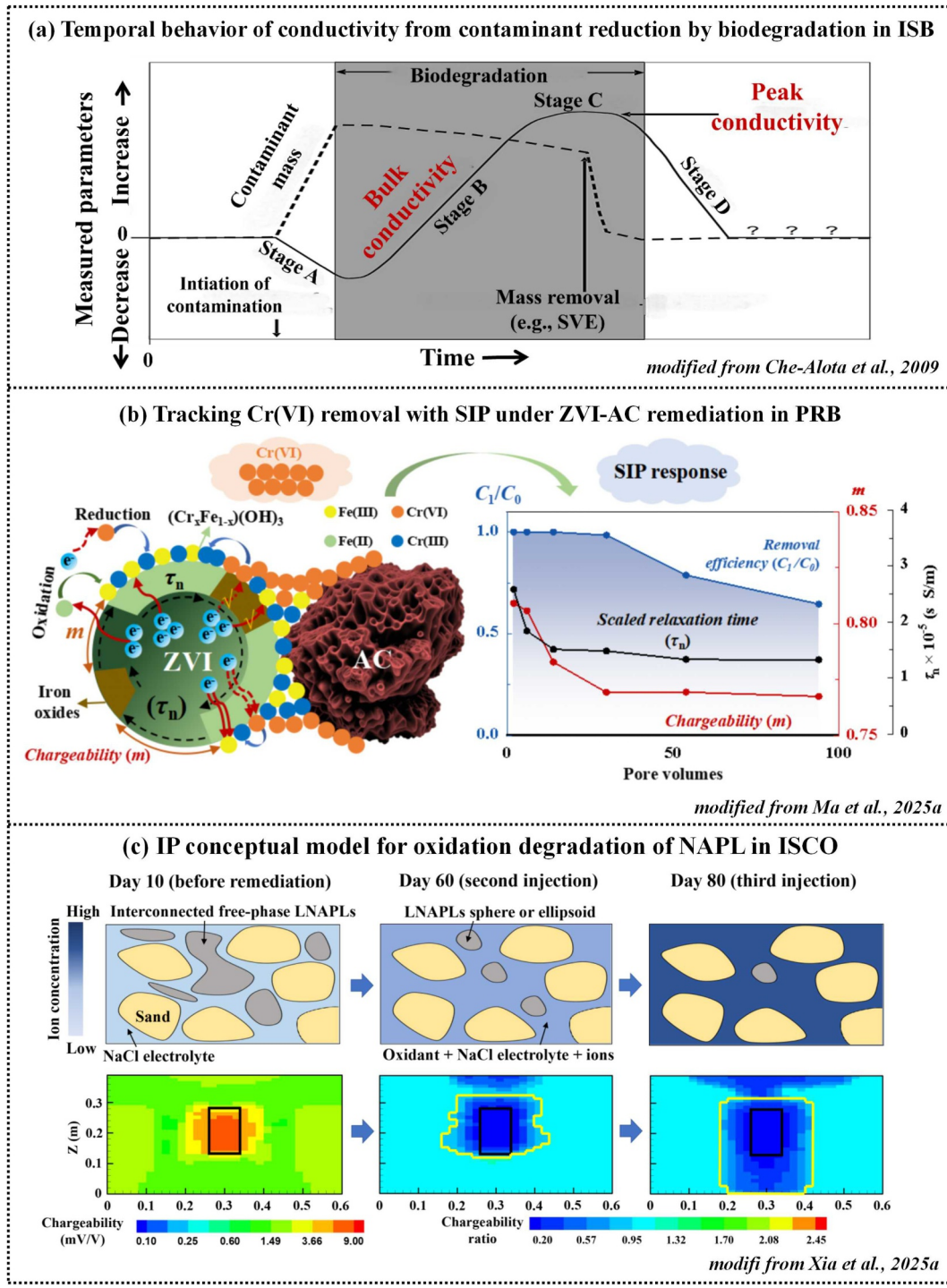

Figure 8. Influences of contaminant on electrical parameters monitoring in situ remediation processes. Changes in concentration, distribution, and phase of contaminant within pore spaces during remediation, coupled with physicochemical or biological environmental alterations (e.g., Che-Alota et al., 2009; Ma, Zhang, et al., 2025; Xia et al., 2025a), increase the complexity of electrical responses.

of electrical parameters, as changes may arise from various simultaneous processes, such as mineral precipitation or alterations in fluid chemistry (Jiang et al., 2014). While this ambiguity complicates the interpretation of static surveys, time-lapse monitoring may address the issue by focusing on temporal variations. Consequently, the electrical parameters must be correlated with ground-truth data (e.g., from borehole sampling or direct-push

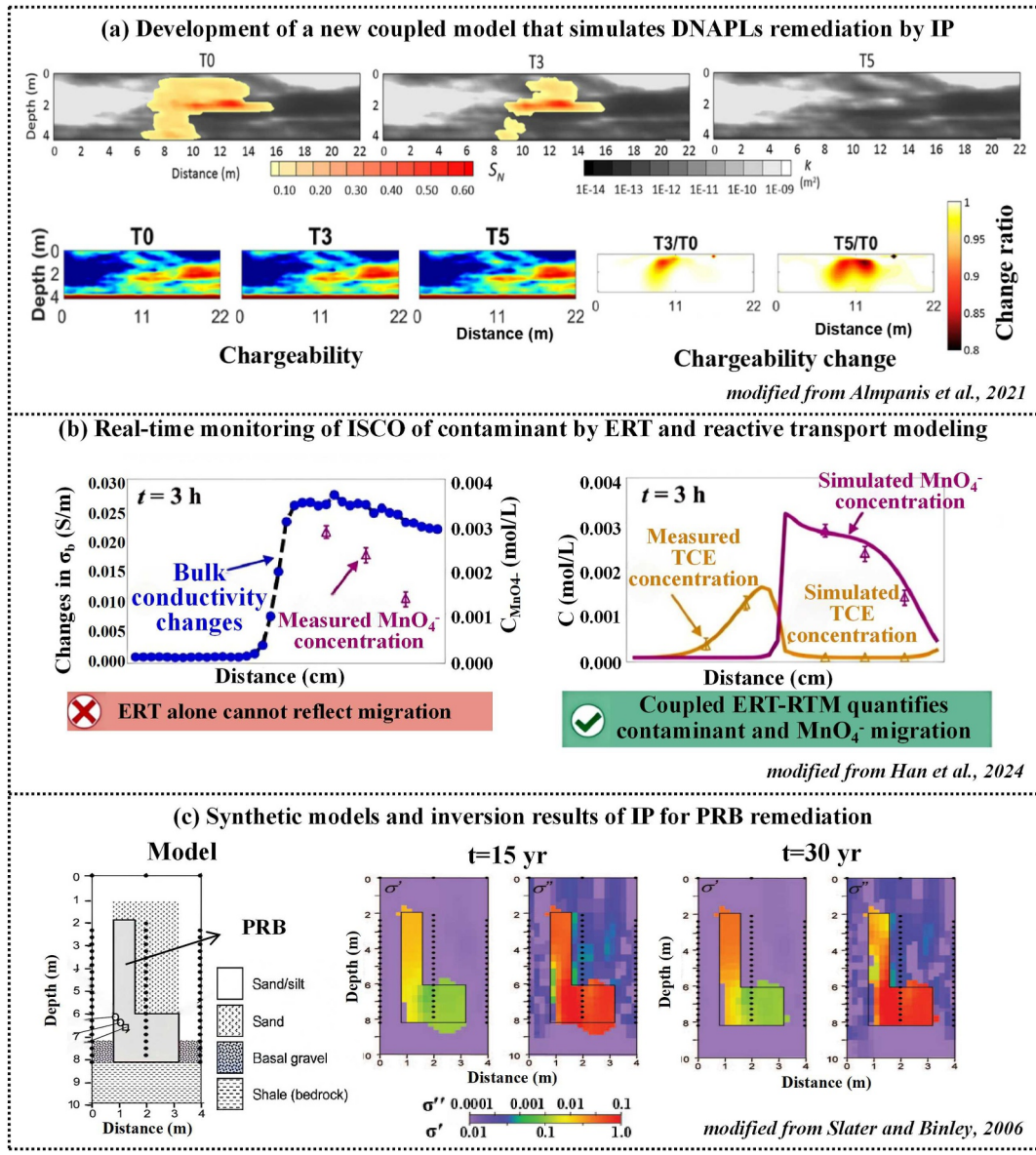

Figure 9. Synthetic studies for in situ remediation process associated with electrical geophysical methods. Integrating electrical response with numerical modeling to rapidly simulate and predict the contaminant removal may provide a robust theoretical basis for optimizing both the application and interpretation of geophysical monitoring.

sensing) to facilitate timely adjustments to remediation strategies and ensure long-term sustainability of the remediation process (Sanuade et al., 2022).

This integrated approach is crucial for the timely adjustment of remediation strategies and ensuring the sustainability of the remediation effect. Specifically, for ISCO/ISCR process, variations in electrical parameters can guide optimization of remediation strategies by adjusting injection locations and volumes, thereby minimizing oxidant waste and preventing secondary pollution (e.g., Han et al., 2024). For the ISB process, microbial activity zones can be accurately delineated using electrical parameter distributions, thus enabling timely remediation progress assessment (e.g., Nivorlis et al., 2024). For ISTR processes, electrical geophysical methods can guide fixed-depth heating to optimize heating strategies, allowing for more reduced energy expenditure (e.g., Xia et al., 2025c). For PRB remediation, electrical geophysical methods can be employed to monitor spatial and temporal variations in electrical responses inside and outside the barrier, which can be used to infer changes in hydraulic properties and assess reactive material longevity (e.g., Hao, Ye, et al., 2021). Consequently, the optimal

monitoring framework integrates geophysical methods to enable real-time and spatially continuous delineation of subsurface processes, while strategically deploying direct sampling to validate critical changes in hydrological and geochemical conditions. This approach minimizes investigation costs while simultaneously enhancing the accuracy and long-term sustainability of remediation efforts.

6. Challenges in Electrical Monitoring of in Situ Remediation Processes

Despite the significant developments in both experimental and field aspects of geophysical monitoring for in situ remediation processes, as illustrated above, many challenges remain as we seek to better understand the effects of hydrogeology, temperature, hydrochemistry, and contaminants on electrical parameters during the remediation process. Based on the application of electrical geophysical methods in monitoring in situ remediation processes, current challenges are primarily encountered during three key stages: pre-monitoring preparations, data collection, data processing and interpretation. We highlight several key challenges for electrical monitoring of in situ remediation during these three stages (Figure 10).

6.1. Resource and Logistical Constraints in Equipment Deployment

Reliable equipment is essential for acquiring high-quality geophysical data to assess remediation effectiveness, whether through single surveys or continuous monitoring. Consequently, equipment acquisition and maintenance costs are one of the key constraints (Takata et al., 2005). However, since electrical methods can significantly reduce the expenses associated with monitoring wells, geophysical data acquisition may offset these costs. In addition, ensuring a reliable and adequate power supply for continuous or long-term geophysical monitoring is critical yet challenging (Chambers et al., 2022), especially in remote sites common to many ISB or PRB implementations. Thus, adopting low power monitoring technology alongside the utilization of sustainable power sources such as solar energy may present a viable solution for many sites. An additional potential challenge involves cable and electrode loss, which is often accelerated by harsh chemical environments encountered during in situ chemical remediation (e.g., corrosive oxidants/reductants) or elevated temperatures in thermal treatments (Tao et al., 2025). However, this challenge has not emerged as a significant issue in practical applications. Finally, deploying automated systems provides a robust alternative to manual surveys by mitigating transport risks while reducing reliance on manual labor and long-term operational costs.

6.2. Complex Subsurface Conditions

The geophysical data acquisition process can influence the accuracy and reliability of monitoring results (Huang & Yang, 2022). Hydrogeological conditions including heterogeneity, along with dynamically evolving subsurface temperature, chemical, and biological environments during remediation, collectively compromise signal quality (Amadi et al., 2024). Nevertheless, as demonstrated in Section 4, understanding the impact of stratum heterogeneity on data collection, coupled with quantitative links between electrical parameters and key hydrogeologic or biological and chemical properties, enables accurate delineation of the remediation processes and their effectiveness. Furthermore, both engineered installations (e.g., injection wells or heaters) and anthropogenic structures (e.g., subsurface pipelines or storage tanks) may interfere with the data collection process (e.g., Meng et al., 2022; Qiang et al., 2025). As illustrated in Figure 4, such interference can be mitigated by adjusting the location of the monitoring lines.

6.3. Non-Uniqueness of Inversion

In general, the inversion of geophysical data is challenging due to non-uniqueness, i.e., multiple subsurface models can satisfy the same acquired data (e.g., Linde et al., 2015; Zhang, Nawaz, et al., 2021). Accordingly, the introduction of regularization functions to address the non-uniqueness of inverse problems by minimizing the roughness of an image has significantly enhanced the robustness of geophysical inverse codes. This made it possible for some geophysical methods, especially electrical geophysical methods, to be widely used in various survey configurations/applications. Furthermore, a critical balance exists between depth penetration and spatial resolution, for example, increasing the surface electrode spacing will increase signal strength and depth of investigation at the expense of reduced resolution (Binley & Slater, 2020). This poses a particular challenge when delineating contaminant variations coupled with dynamic subsurface environments during remediation.

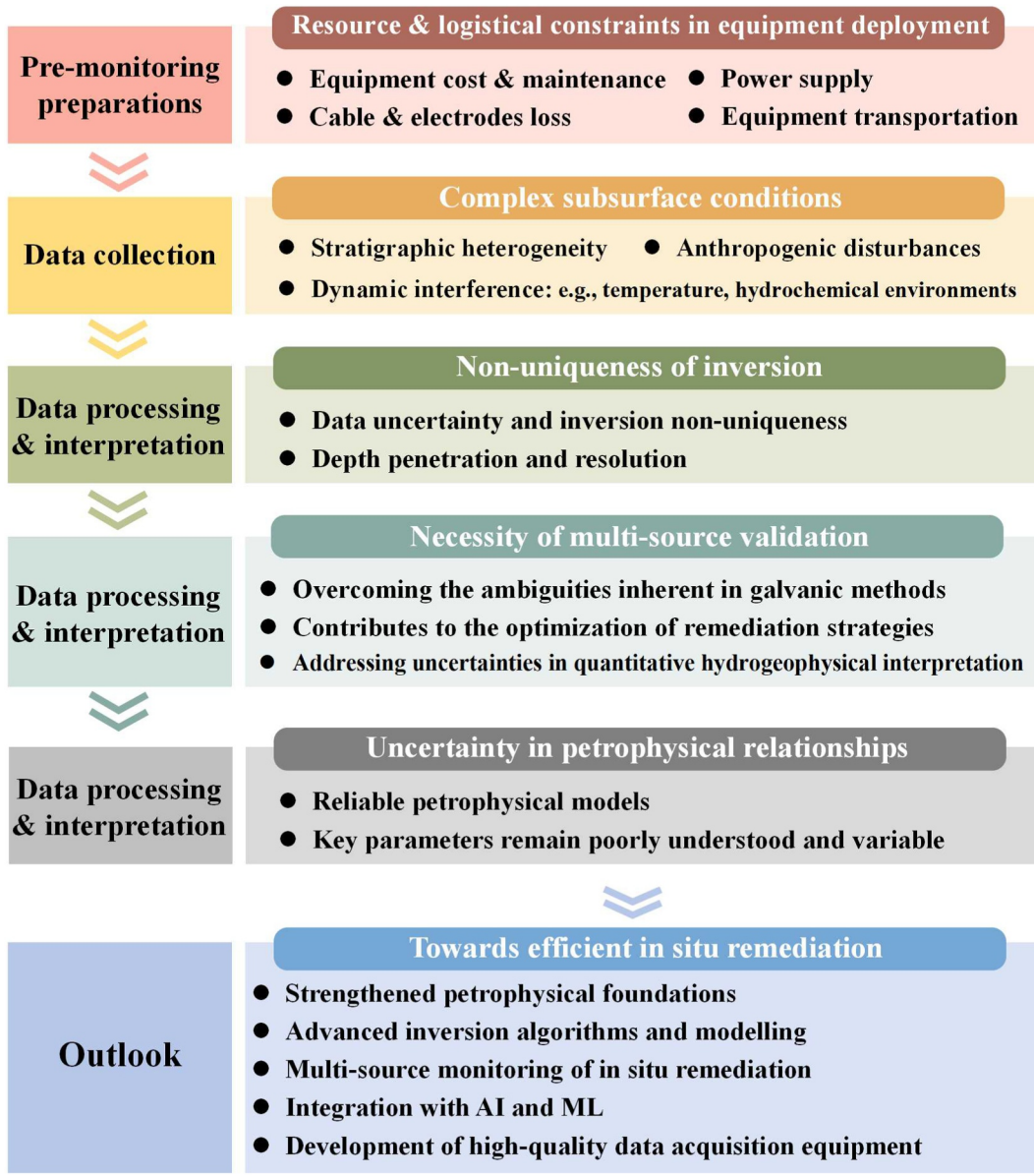

Figure 10. Challenges and outlook with respect to electrical monitoring of in situ remediation.

Optimizing the array protocols based on site-specific conditions may provide an effective solution to the challenges mentioned above.

6.4. Necessity of Multi-Source Validation

Geophysical data interpretation requires integration with multi-source validation data—including hydrogeological/hydrochemical parameters and contaminant distribution—to reduce uncertainty (e.g., Alao et al., 2025; Binley et al., 2015; Liao et al., 2018). As discussed in the following section, the inherent uncertainty in petrophysical relationships further underscores the need for such integration. Site-specific information is essential for optimal design of monitoring survey lines, particularly given the inherent resolution limitations of individual electrical parameters in delineating subsurface dynamics during remediation. Geophysical monitoring and other analytical methods can be integrated to enable real-time monitoring of changes in the subsurface environment during the remediation process. Crucially, electrical parameters function as early warning indicators for detecting subsurface anomalies that require direct sampling, particularly during transient events like abrupt

rainfall that alter hydrologic conditions. This decision-support capability enables targeted sampling of hydrochemical parameters and contaminants when geophysical monitoring detects critical subsurface changes, thereby optimizing remediation strategies in real time while controlling investigation costs.

6.5. Uncertainty in Petrophysical Relationships

A further challenge lies in the translation of geophysical images into parameters directly relevant to remediation performance, such as contaminant concentration or reagent distribution. This translation relies on petrophysical relationships linking electrical properties to subsurface states. However, as highlighted by Binley and Slater (2020), reliable petrophysical models, particularly under unsaturated conditions, remain lacking in the community, forcing practitioners to rely on empirical or semi-empirical relations with numerous poorly constrained parameters. This uncertainty is especially critical during remediation, where pore fluid chemistry, saturation, and surface properties evolve simultaneously. However, few authors have attempted to explore the importance of petrophysical uncertainty on the interpretation of electrical geophysical images (but see Brunetti & Linde, 2017; Tso et al., 2019). For example, separating the contributions of reagent injection from contaminant degradation to bulk conductivity changes requires knowledge of the relative contributions of electrolytic conduction (representing ion transport in pore fluids) and surface conduction (associated with the electrical double layer at mineral-fluid interfaces)—parameters that may themselves alter during treatment. Similarly, while induced polarization shows promise for tracking mineral precipitation or biofilm growth, the empirical correlations linking polarization parameters to these processes often require site-specific calibration and may not transfer across different lithologies or geochemical environments.

7. Outlook

To promote the efficient advancement of in situ remediation, future research efforts in geophysical monitoring should focus on (Figure 10):

1. Strengthened petrophysical foundations are needed to enable quantitative interpretation under remediation-specific conditions. Advancing this front will require integrated laboratory and field studies that constrain the relationships between electrical properties and key remediation metrics (e.g., contaminant concentration, reagent distribution, microbial activity) across diverse lithologies and geochemical environments. Such foundational work is essential for transforming geophysical signatures from qualitative indicators into quantitative measures of remediation performance.
2. While advanced inversion algorithms already enable high-resolution imaging of dynamic remediation processes, it is necessary to better understand the relationship between geophysical properties and temperature, hydrological conditions, and hydrochemical properties, and, in some cases, to perform inversion in a coupled manner, that is, to generate parameter proposals using a multi-field coupled model and to assess the uncertainty within the models. Thus, the multi-field model constrains the inversion, thereby guaranteeing that the final results align with the conceptual understanding of hydrological, hydrochemical, or other relevant field conditions.
3. Multi-source monitoring frameworks that synergize electrical parameters with temperature and hydrochemical sensors. Such integration is critical to track reagent delivery efficiency in chemical remediation, biological activity changes in ISB process, heat conduction process during ISTR, and reactive zone longevity in PRB, thereby correlating geophysical signatures with specific remediation mechanisms.
4. Artificial intelligence (AI) and machine learning (ML) offer transformative potential in two key areas, that is, inversion and interpretation. AI/ML techniques can be robust where established models fail, as they can solve complex problems without relying on potentially violated assumptions. Beyond inversion, these models excel at interpretation by learning directly from data to integrate geophysical measurements with remediation performance metrics. These models enable real-time forecasting of contaminant degradation processes, optimize injection strategies for chemical/biological amendments, control thermal source deployment, and diagnose PRB longevity.
5. Development of multi-source information monitoring platform for in situ remediation processes, providing real-time delineation of the remediation process and data-driven guidance for strategy optimization (Figure 11). Such a platform would provide unparalleled insights into the complex spatial-temporal dynamics of remediation processes. Specifically, such an autonomous system would continuously integrate electrical responses with critical parameters (e.g., temperature, hydrochemical data) to detect subsurface anomalies that

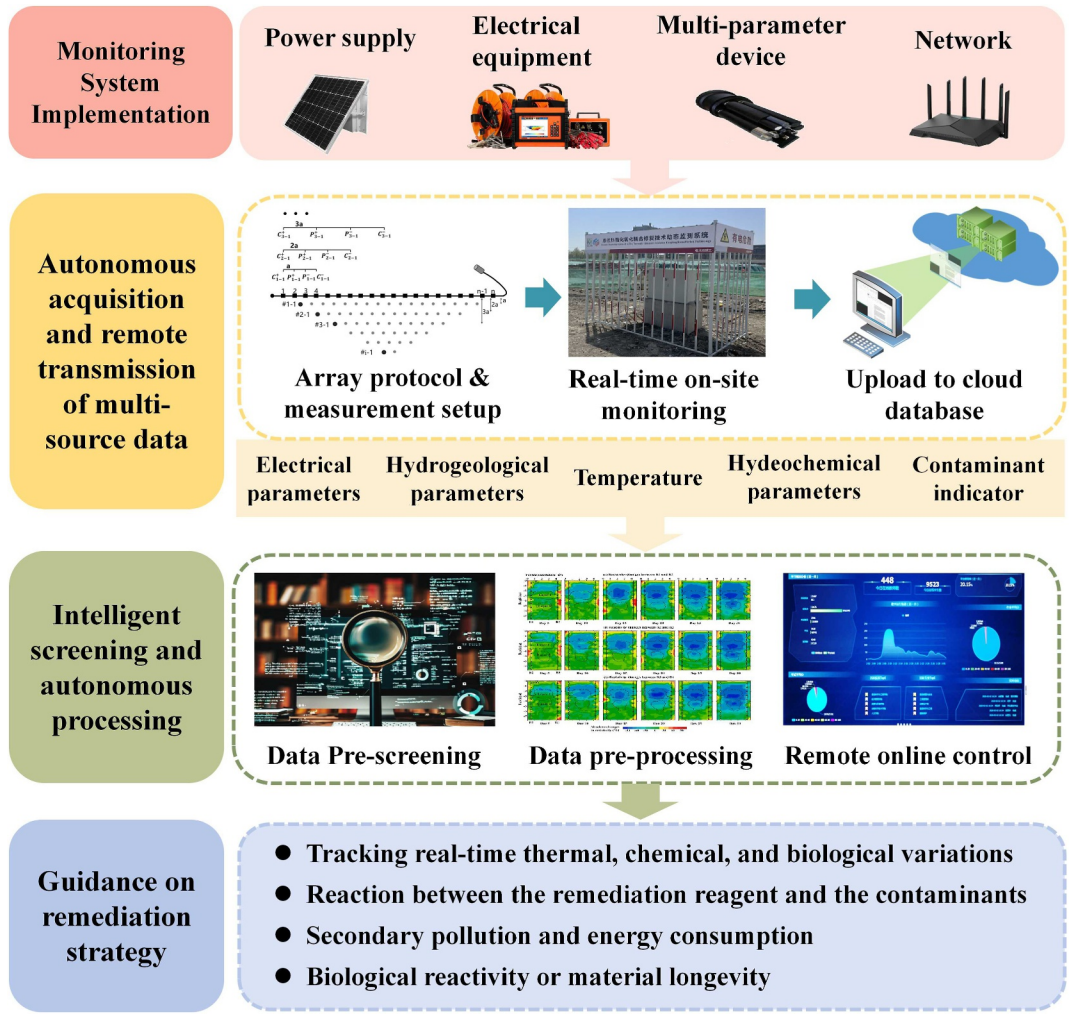

Figure 11. A conceptual framework for a multi-source information monitoring platform centered on electrical geophysical methods.

prompt targeted sampling during transient events such as rainfall-induced hydraulic disturbances, a capability that remains an emerging frontier where recent advances have demonstrated its potential for real-time remediation management (Johnson et al., 2022). Such a feature would enable real-time remediation adjustments, such as modifying injection points to ensure that reaction reagents reach contaminant plumes, thereby transforming geophysical monitoring data into active remediation control actions.

8. Closing Remarks

We have reviewed advances in using ERT/IP to monitor four remediation technologies: ISCO/ISCR, ISB, ISTR, and PRB. Electrical methods effectively track subsurface changes in hydrogeology, temperature, hydrochemistry, and contaminant distribution. Their key contribution is providing spatially continuous proxy data that enables targeted sampling while reducing investigation costs.

For remediation management, electrical imaging enables real-time visualization of reagent transport, microbial activity zones, heat distribution, and barrier integrity. Integrated with direct measurements, these electrical-process correlations support quantitative interpretation of reagent distribution, microbial transformations, temperature evolution, and material reactivity.

Linking geophysical responses to specific remediation processes remains challenging due to parameter non-uniqueness and site heterogeneity. Overcoming these barriers requires robust petrophysical relationships,

coupled inversion frameworks, multi-source data integration, and AI/ML to enable predictive, adaptive remediation strategies. By bridging the gap between geophysical data and process-based understanding, these methods enable more efficient, data-driven remediation strategies.

Conflict of Interest

The authors declare no conflicts of interest relevant to this study.

Availability Statement

The data used in this study are available in the Zenodo repository at Xia (2025).

Acknowledgments
The first author, Dr. Xia thanks the support of National Science Foundation (42407067) and China Postdoctoral Science Foundation (2024M751710). The corresponding author also acknowledges the support from the National Science Foundation (42177056).

References

Alao, J. O., Balarabe, B., Ayejoto, D. A., Abubakar, F., Otorkpa, O. J., & Eze, S. U. (2025). Evaluation of hydrocarbon and co-contaminants in groundwater and associated public health risks using electrical resistivity and hydrochemical data. *Water Resources and Industry*, *34*, 100319. https://doi.org/10.1016/j.wri.2025.100319

Alao, J. O., Lawal, K. M., Dewu, B. B. M., & Raimi, J. (2024). Detection of shallow underground targets using electrical resistivity tomography and the implications in civil/environmental engineering. *Discover Geoscience*, *2*(1), 52. https://doi.org/10.1007/s44288-024-00058-6

Almpanis, A., Gerhard, J., & Power, C. (2021). Mapping and monitoring of DNAPL source zones with combined direct current resistivity and induced polarization: A Field-Scale Numerical Investigation. *Water Resources Research*, *57*(11), e2021WR031366. https://doi.org/10.1029/2021wr031366

Almpanis, A., Slater, L., Gerhard, J. I., & Power, C. (2023). Spectral induced polarization signatures of smoldering remediation enhanced with colloidal activated carbon: An experimental study. *Journal of Contaminant Hydrology*, *259*, 104266. https://doi.org/10.1016/j.jconhyd.2023.104266

Amadi, A. H., Ajienka, J. A., Akaranta, O., Moses, P. R., Achara, N. U., Ola, V. D., & Udo, R. D. (2024). A review of soil resistivity testing for enhanced corrosion control: Overcoming limitations through integrated geophysical approaches and alternative methodologies. *Measurement*, *242*, 116214. https://doi.org/10.1016/j.measurement.2024.116214

Archie, G. (1942). The electrical resistivity log as an aid in determining some reservoir characteristics. *Transactions of the AIME*, *146*(1), 54–62. https://doi.org/10.2118/942054-g

Atekwana, E. A., & Atekwana, E. A. (2010). Geophysical signatures of microbial activity at hydrocarbon contaminated sites: A review. *Surveys in Geophysics*, *31*(2), 247–283. https://doi.org/10.1007/s10712-009-9089-8

Atekwana, E. A., Atekwana, E. A., Rowe, R. S., Werkema, D. D., & Legall, F. D. (2004). The relationship of total dissolved solids measurements to bulk electrical conductivity in an aquifer contaminated with hydrocarbon. *Journal of Applied Geophysics*, *56*(4), 281–294. https://doi.org/10.1016/j.jappgeo.2004.08.003

Atekwana, E. A., Atekwana, E. A., Werkema, D. D., Allen, J. P., Smart, L. A., Duris, J. W., et al. (2004b). Evidence for microbial enhanced electrical conductivity in hydrocarbon-contaminated sediments. *Geophysical Research Letters*, *31*(23), L23501. https://doi.org/10.1029/2004gl021359

Bate, B., Ye, J., Cao, J., You, Y., Cao, J., Zhang, S., et al. (2022). The mechanisms and monitoring of zeolite remediating chemical oxygen demand, NH^{4+}, and Pb^{2+}. *Journal of Applied Geophysics*, *199*, 104615. https://doi.org/10.1016/j.jappgeo.2022.104615

Binley, A., Hubbard, S. S., Huisman, J. A., Revil, A., Robinson, D. A., Singha, K., & Slater, L. D. (2015). The emergence of hydrogeophysics for improved understanding of subsurface processes over multiple scales. *Water Resources Research*, *51*(6), 3837–3866. https://doi.org/10.1002/2015wr017016

Binley, A., & Slater, L. (2020). *Resistivity and induced polarization*. Cambridge University Press. https://doi.org/10.1017/9781108685955

Bording, T., Kühl, A. K., Fiandaca, G., Christensen, J. F., Christiansen, A. V., & Auken, E. (2020). Cross-borehole geoelectrical time-lapse monitoring of in situ chemical oxidation and permeability estimation through induced polarization. *Near Surface Geophysics*, *19*(1), 43–58. https://doi.org/10.1002/nsg.12131

Brunetti, C., & Linde, N. (2017). Impact of petrophysical uncertainty on Bayesian hydrogeophysical inversion and model selection. *Advances in Water Resources*, *111*, 346–359. https://doi.org/10.1016/j.advwatres.2017.11.028

Budania, R., & Dangayach, S. (2023). A comprehensive review on permeable reactive barrier for the remediation of groundwater contamination. *Journal of Environmental Management*, *332*, 117343. https://doi.org/10.1016/j.jenvman.2023.117343

Caterina, D., Orozco, A. F., & Nguyen, F. (2017). Long-term ERT monitoring of biogeochemical changes of an aged hydrocarbon contamination. *Journal of Contaminant Hydrology*, *201*, 19–29. https://doi.org/10.1016/j.jconhyd.2017.04.003

Chambers, J., Holmes, J., Whiteley, J., Boyd, J., Meldrum, P., Wilkinson, P., et al. (2022). Long-term geoelectrical monitoring of landslides in natural and engineered slopes. *The Leading Edge*, *41*(11), 768–776. https://doi.org/10.1190/tle41110768.1

Chambers, J., Wilkinson, P., Wealthall, G., Loke, M., Dearden, R., Wilson, R., et al. (2010). Hydrogeophysical imaging of deposit heterogeneity and groundwater chemistry changes during DNAPL source zone bioremediation. *Journal of Contaminant Hydrology*, *118*(1–2), 43–61. https://doi.org/10.1016/j.jconhyd.2010.07.001

Che-Alota, V., Atekwana, E. A., Atekwana, E. A., Sauck, W. A., & Werkema, D. D. (2009). Temporal geophysical signatures from contaminant-mass remediation. *Geophysics*, *74*(4), B113–B123. https://doi.org/10.1190/1.3139769

Chen, H., Park, E., & Hu, C. (2018). A design solution of PRB with multispecies transport based on a multi-domain system. *Environmental Earth Sciences*, *77*(18), 630. https://doi.org/10.1007/s12665-018-7804-9

Chen, J., Hsu, S., Li, M., & Liu, C. (2016). Assessing the performance of a permeable reactive barrier–aquifer system using a dual-domain solute transport model. *Journal of Hydrology*, *543*, 849–860. https://doi.org/10.1016/j.jhydrol.2016.11.002

Chen, J., Hubbard, S. S., & Williams, K. H. (2013). Data-driven approach to identify field-scale biogeochemical transitions using geochemical and geophysical data and hidden Markov models: Development and application at a uranium-contaminated aquifer. *Water Resources Research*, *49*(10), 6412–6424. https://doi.org/10.1002/wrcr.20524

Ciampi, P., Cassiani, G., Deidda, G. P., Esposito, C., Rizzetto, P., Pizzi, A., & Papini, M. P. (2024). Understanding the dynamics of enhanced light non-aqueous phase liquids (LNAPL) remediation at a polluted site: Insights from hydrogeophysical findings and chemical evidence. *The Science of the Total Environment*, *932*, 172934. https://doi.org/10.1016/j.scitotenv.2024.172934

Cole, K., & Cole, R. (1941). Dispersion and absorption in dielectrics I. Alternating Current properties. *Journal of Chemical Physics*, *9*(4), 341–351. https://doi.org/10.1063/1.1750906

Colombano, S., Davarzani, H., Van Hullebusch, E. D., Ignatiadis, I., Huguenot, H., Zornig, C., & Guyonnet, D. (2020). In situ Thermal Treatments and enhancements: Theory and case study. In *Applied environmental science and engineering for a sustainable future* (pp. 149–209). https://doi.org/10.1007/978-3-030-40348-5_3

Conrad, M. E., Brodie, E. L., Radtke, C. W., Bill, M., Delwiche, M. E., Lee, M. H., et al. (2010). Field evidence for Co-Metabolism of trichloroethene stimulated by addition of electron donor to groundwater. *Environmental Science and Technology*, *44*(12), 4697–4704. https://doi.org/10.1021/es903535j

Cundy, A. B., Hopkinson, L., & Whitby, R. L. (2008). Use of iron-based technologies in contaminated land and groundwater remediation: A review. *The Science of the Total Environment*, *400*(1–3), 42–51. https://doi.org/10.1016/j.scitotenv.2008.07.002

Dahlin, T., & Leroux, V. (2012). Improvement in time-domain induced polarization data quality with multi-electrode systems by separating current and potential cables. *Near Surface Geophysics*, *10*(6), 545–565. https://doi.org/10.3997/1873-0604.2012028

Dahlin, T., & Loke, M. H. (2018). Underwater ERT surveying in water with resistivity layering with example of application to site investigation for a rock tunnel in central Stockholm. *Near Surface Geophysics*, *16*(3), 230–237. https://doi.org/10.3997/1873-0604.2018007

Davis, C. A., Atekwana, E., Atekwana, E., Slater, L. D., Rossbach, S., & Mormile, M. R. (2006). Microbial growth and biofilm formation in geologic media is detected with complex conductivity measurements. *Geophysical Research Letters*, *33*(18). https://doi.org/10.1029/2006gl027312

Davis, C. A., Slater, L. D., Kulessa, B., Ferguson, A. S., Atekwana, E. A., Doherty, R., & Kalin, R. (2010). Self-potential signatures associated with an injection experiment at an in situ biological permeable reactive barrier. *Near Surface Geophysics*, *8*(6), 541–551. https://doi.org/10.3997/1873-0604.2010034

Davis, E. L. (2023). In *In situ thermal remediation*. United States Environmental Protection Agency. EPA/600/R-23/062 Retrieved from https://cluin.org/download/techfocus/thermal/Insitu-Thermal-Remediation.pdf

Day-Lewis, F. D., Slater, L. D., Robinson, J., Johnson, C. D., Terry, N., & Werkema, D. (2017). An overview of geophysical technologies appropriate for characterization and monitoring at fractured-rock sites. *Journal of Environmental Management*, *204*, 709–720. https://doi.org/10.1016/j.jenvman.2017.04.033

Del Reino, S., Rodríguez-Rastrero, M., Escolano, O., Welte, L., Bueno, J., Fernández, J. L., et al. (2014). In situ chemical oxidation based on hydrogen peroxide: Optimization of its application to an hydrocarbon polluted site. In *The handbook of environmental chemistry* (pp. 207–228). https://doi.org/10.1007/698_2014_272

Ding, D., Song, X., Wei, C., & LaChance, J. (2019). A review on the sustainability of thermal treatment for contaminated soils. *Environmental Pollution*, *253*, 449–463. https://doi.org/10.1016/j.envpol.2019.06.118

Doherty, R., Kulessa, B., Ferguson, A. S., Larkin, M. J., Kulakov, L. A., & Kalin, R. M. (2010). A microbial fuel cell in contaminated ground delineated by electrical self-potential and normalized induced polarization data. *Journal of Geophysical Research*, *115*(G3). https://doi.org/10.1029/2009jg001131

Edwards, L. S. (1977). A modified pseudosection for resistivity and IP. *Geophysics*, *42*(5), 1020–1036. https://doi.org/10.1190/1.1440762

Eggleston, J., & Rojstaczer, S. (1998). Identification of large-scale hydraulic conductivity trends and the influence of trends on contaminant transport. *Water Resources Research*, *34*(9), 2155–2168. https://doi.org/10.1029/98wr01475

Elder, C. R., & Benson, C. H. (2018). Performance and economic comparison of PRB types in heterogeneous aquifers. *Environmental Geotechnics*, *6*(4), 214–224. https://doi.org/10.1680/jenge.17.00063

Elshall, A. S., Arik, A. D., El-Kadi, A. I., Pierce, S., Ye, M., Burnett, K. M., et al. (2020). Groundwater sustainability: A review of the interactions between science and policy. *Environmental Research Letters*, *15*(9), 093004. https://doi.org/10.1088/1748-9326/ab8e8c

Environmental Protection Agency (EPA). (2013). Introduction to in situ bioremediation of groundwater. Washington, DC Retrieved from https://semspub.epa.gov/work/HQ/171054.pdf

Environmental Protection Agency (EPA). (2023). Superfund remedy report (17th ed.). Retrieved from https://www.epa.gov/remedytech/superfund-remedy-report

Flores Orozco, A., Micić, V., Bücker, M., Gallistl, J., Hofmann, T., & Nguyen, F. (2019). Complex-conductivity monitoring to delineate aquifer pore clogging during nanoparticles injection. *Geophysical Journal International*, *218*(3), 1838–1852. https://doi.org/10.1093/gji/ggz255

Flores Orozco, A., Velimirovic, M., Tosco, T., Kemna, A., Sapion, H., Klaas, N., et al. (2015). Monitoring the injection of microscale zerovalent iron particles for groundwater remediation by means of complex electrical conductivity imaging. *Environmental Science and Technology*, *49*(9), 5593–5600. https://doi.org/10.1021/acs.est.5b00208

Florsch, N., Llubes, M., Téreygeol, F., Ghorbani, A., & Roblet, P. (2011). Quantification of slag heap volumes and masses through the use of induced polarization: Application to the Castel-Minier site. *Journal of Archaeological Science*, *38*(2), 438–451. https://doi.org/10.1016/j.jas.2010.09.027

Gavaskar, A., Sass, B., Gupta, N., Drescher, E., Yoon, W.-S., Sminchak, J., et al. (2002). Evaluating the longevity and hydraulic performance of permeable reactive barriers at department of defense sites.

Gibert, O., Pomierny, S., Rowe, I., & Kalin, R. M. (2008). Selection of organic substrates as potential reactive materials for use in a denitrification permeable reactive barrier (PRB). *Bioresource Technology*, *99*(16), 7587–7596. https://doi.org/10.1016/j.biortech.2008.02.012

Griffiths, D. R. (2020). Controlling secondary pollution impacts during enhanced in situ anaerobic bioremediation. *Elsevier eBooks*, 201–220. https://doi.org/10.1016/b978-0-12-817982-6.00008-2

Grotenhuis, T. J., & Rijnaarts, H. H. (2011). *In situ remediation technologies* (pp. 949–977). Springer eBooks. https://doi.org/10.1007/978-90-481-9757-6_21

Halihan, T., Albano, J., Comfort, S. D., & Zlotnik, V. A. (2012). Electrical resistivity imaging of a permanganate injection during in situ treatment of RDX-Contaminated groundwater. *Groundwater Monitoring & Remediation*, *32*(1), 43–52. https://doi.org/10.1111/j.1745-6592.2011.01361.x

Han, Z., Kang, X., Singha, K., Wu, J., & Shi, X. (2024). Real-time monitoring of in situ chemical oxidation (ISCO) of dissolved TCE by integrating electrical resistivity tomography and reactive transport modeling. *Water Research*, *252*, 121195. https://doi.org/10.1016/j.watres.2024.121195

Hao, N., Cao, J., Ye, J., Zhang, C., Li, C., & Bate, B. (2021). Content and morphology of lead remediated by activated carbon and biochar: A spectral induced polarization study. *Journal of Hazardous Materials*, *411*, 124605. https://doi.org/10.1016/j.jhazmat.2020.124605

Hao, N., Ye, J. S., Zhao, L., Sun, M., You, Y. Q., Zhang, C., et al. (2021). Evaluating iron remediation with limestone using spectral induced polarization and microscopic techniques. *The Science of the Total Environment*, *800*, 149641. https://doi.org/10.1016/j.scitotenv.2021.149641

Harte, P. T., Smith, T. E., Williams, J. H., & Degnan, J. R. (2012). Time series geophysical monitoring of permanganate injections and in situ chemical oxidation of PCE, OU1 area, Savage Superfund Site, Milford, NH, USA. *Journal of Contaminant Hydrology*, *132*, 58–74. https://doi.org/10.1016/j.jconhyd.2012.01.008

Hayley, K., Pidlisecky, A., & Bentley, L. (2011). Simultaneous time-lapse electrical resistivity inversion. *Journal of Applied Geophysics*, *75*(2), 401–411. https://doi.org/10.1016/j.jappgeo.2011.06.035

Honetschlägerová, L., Martinec, M., & Škarohlíd, R. (2019). Coupling in situ chemical oxidation with bioremediation of chloroethenes: A review. *Reviews in Environmental Science and Bio/Technology*, *18*(4), 699–714. https://doi.org/10.1007/s11157-019-09512-1

Horst, J., Munholland, J., Hegele, P., Klemmer, M., & Gattenby, J. (2021). In situ thermal remediation for source areas: Technology advances and a review of the market from 1988–2020. *Groundwater Monitoring & Remediation*, *41*(1), 17–31. https://doi.org/10.1111/gwmr.12424

Hort, R. D., Revil, A., & Munakata-Marr, J. (2014). Analysis of sources of bulk conductivity change in saturated silica sand after unbuffered TCE oxidation by permanganate. *Journal of Contaminant Hydrology*, *165*, 11–23. https://doi.org/10.1016/j.jconhyd.2014.07.003

Hort, R. D., Revil, A., Munakata-Marr, J., & Mao, D. (2015). Evaluating the potential for quantitative monitoring of in situ chemical oxidation of aqueous-phase TCE using in-phase and quadrature electrical conductivity. *Water Resources Research*, *51*(7), 5239–5259. https://doi.org/10.1002/2014wr016868

Hou, D., Al-Tabbaa, A., O'Connor, D., Hu, Q., Zhu, Y., Wang, L., et al. (2023). Sustainable remediation and redevelopment of brownfield sites. *Nature Reviews Earth and Environment*, *4*(4), 271–286. https://doi.org/10.1038/s43017-023-00404-1

Hou, D., & O'Connor, D. (2020). *Green and sustainable remediation: Past, present, and future developments* (pp. 19–42). Elsevier eBooks. https://doi.org/10.1016/b978-0-12-817982-6.00002-1

Huang, L., & Yang, X. (2022). *Evaluating different geophysical monitoring techniques for geological carbon storage* (pp. 1–7). Geophysical Monograph. https://doi.org/10.1002/9781119156871.ch1

Huling, S. G., & Pivetz, B. E. (2006). In *-Situ chemical oxidation*. United States Environmental Protection Agency. EPA/600/R-06/072 Retrieved from https://clu-in.org/download/contaminantfocus/pcb/ISCO-600R06072.pdf

Hussain, A., Rehman, F., Rafeeq, H., Waqas, M., Asghar, A., Afsheen, N., et al. (2022). In-situ, Ex-situ, and nano-remediation strategies to treat polluted soil, water, and air – A review. *Chemosphere*, *289*, 133252. https://doi.org/10.1016/j.chemosphere.2021.133252

Interstate Technology and Regulatory Council (ITRC). (2011). Permeable reactive barrier: Technology update. Washington, DC Retrieved from https://itrcweb.org/wp-content/uploads/2024/09/PRB-5-1.pdf

Iravani, M. A., Davarzani, H., Deparis, J., Colombano, S., Philippe, N., Oniangue, B., et al. (2022). Experimental study of electrical complex resistivity in a 2D multiphase porous medium under non-isothermal conditions: Application to soil remediation monitoring. *Near Surface Geophysics*, *21*(1), 65–81. https://doi.org/10.1002/nsg.12237

Iravani, M. A., Deparis, J., Davarzani, H., Colombano, S., Guérin, R., & Maineult, A. (2020). The influence of temperature on the dielectric permittivity and complex electrical resistivity of porous media saturated with DNAPLs: A laboratory study. *Journal of Applied Geophysics*, *172*, 103921. https://doi.org/10.1016/j.jappgeo.2019.103921

Ismail, R. E., Al-Raoush, R. I., & Alazaiza, M. Y. D. (2023). The impact of water table fluctuation and salinity on LNAPL distribution and geochemical properties in the smear zone under completely anaerobic conditions. *Environmental Earth Sciences*, *82*(15), 368. https://doi.org/10.1007/s12665-023-11051-6

Jia, W., Deng, Z., Papini, M. P., Cheng, L., Jin, N., Zhang, D., et al. (2025). Long-term response mechanism of bacterial communities to chemical oxidation remediation in petroleum hydrocarbon contaminated groundwater. *Journal of Hazardous Materials*, *488*, 137239. https://doi.org/10.1016/j.jhazmat.2025.137239

Jiang, X., Wan, L., Wang, J., Yin, B., Fu, W., & Lin, C. (2014). Field identification of groundwater flow systems and hydraulic traps in drainage basins using a geophysical method. *Geophysical Research Letters*, *41*(8), 2812–2819. https://doi.org/10.1002/2014gl059579

Johnson, P., Dahlen, P., Triplett Kingston, J. L., Foote, E., & Williams, S. (2009). Critical evaluation of state-of-the-art in situ thermal treatment technologies for DNAPL source Zone treatment. *ESTCP Project ER-0314, no. May*. https://clu-in.org/download/techfocus/thermal/Thermal-ER-0314-Overview.pdf

Johnson, T. C., Strickland, C., Thomle, J., Day-Lewis, F., & Versteeg, R. (2022). Autonomous time-lapse electrical imaging for real-time management of subsurface systems. *The Leading Edge*, *41*(8), 520–528. https://doi.org/10.1190/tle41080520.1

Johnson, T. C., Versteeg, R. J., Day-Lewis, F. D., Major, W., & Lane, J. W. (2015). Time-lapse electrical geophysical monitoring of Amendment-Based biostimulation. *Ground Water*, *53*(6), 920–932. https://doi.org/10.1111/gwat.12291

Johnson, T. C., Versteeg, R. J., Huang, H., & Routh, P. S. (2009b). Data-domain correlation approach for joint hydrogeologic inversion of time-lapse hydrogeologic and geophysical data. *Geophysics*, *74*(6), 1ND–Z107. https://doi.org/10.1190/1.3237087

Joyce, R. A., Glaser, D. R., Werkema, D. D., & Atekwana, E. A. (2012). Spectral induced polarization response to nanoparticles in a saturated sand matrix. *Journal of Applied Geophysics*, *77*, 63–71. https://doi.org/10.1016/j.jappgeo.2011.11.009

Kang, N., Hua, I., & Rao, P. S. C. (2004). Production and characterization of encapsulated potassium permanganate for sustained release as an in situ oxidant. *Industrial and Engineering Chemistry Research*, *43*(17), 5187–5193. https://doi.org/10.1021/ie0499097

Karandish, F., Liu, S., & De Graaf, I. (2025). Global groundwater sustainability: A critical review of strategies and future pathways. *Journal of Hydrology*, *657*, 133060. https://doi.org/10.1016/j.jhydrol.2025.133060

Karaoulis, M., Kim, J., & Tsourlos, P. (2011). 4D active time constrained resistivity inversion. *Journal of Applied Geophysics*, *73*(1), 25–34. https://doi.org/10.1016/j.jappgeo.2010.11.002

Keller, G. V. (1959). Analysis of some electrical transient measurements on igneous, sedimentary, and metamorphic rocks. In J. R. Wait (Ed.), *Overvoltage research and geophysical applications* (pp. 92–111). Pergamon.

Kemna, A., Binley, A., Cassiani, G., Niederleithinger, E., Revil, A., Slater, L., et al. (2012). An overview of the spectral induced polarization method for near-surface applications. *Near Surface Geophysics*, *10*(6), 453–468. https://doi.org/10.3997/1873-0604.2012027

Kessouri, P., Johnson, T., Day-Lewis, F. D., Wang, C., Ntarlagiannis, D., & Slater, L. D. (2022). Post-remediation geophysical assessment: Investigating long-term electrical geophysical signatures resulting from bioremediation at a chlorinated solvent contaminated site. *Journal of Environmental Management*, *302*, 113944. https://doi.org/10.1016/j.jenvman.2021.113944

Kim, J., Yi, M., Park, S., & Kim, J. G. (2009). 4-D inversion of DC resistivity monitoring data acquired over a dynamically changing earth model. *Journal of Applied Geophysics*, *68*(4), 522–532. https://doi.org/10.1016/j.jappgeo.2009.03.002

Kingston, J. T., Dahlen, P. R., Johnson, P. C., Foote, E., & Williams, S. (2010). Critical evaluation of state-of-the-art in situ thermal treatment technologies for DNAPL source Zone treatment. *ESTCP Project ER-0314, no. January*. https://clu-in.org/download/techfocus/thermal/Thermal-ER-0314-FR.pdf

LaBrecque, D. J., Ramirez, A. L., Daily, W. D., Binley, A. M., & Schima, S. A. (1996). ERT monitoring of environmental remediation processes. *Measurement Science and Technology*, *7*(3), 375–383. https://doi.org/10.1088/0957-0233/7/3/019

LaBrecque, D. J., & Yang, X. (2001). Difference inversion of ERT data: A fast inversion method for 3-D in situ monitoring. *Journal of Environmental & Engineering Geophysics*, *6*(2), 83–89. https://doi.org/10.4133/jeeg6.2.83

Lesmes, D. P., & Frye, K. M. (2001). Influence of pore fluid chemistry on the complex conductivity and induced polarization responses of Berea sandstone. *Journal of Geophysical Research*, *106*(B3), 4079–4090. https://doi.org/10.1029/2000jb900392

Lévy, L., Bording, T. S., Fiandaca, G., Christiansen, A. V., Madsen, L. M., Bennedsen, L. F., et al. (2024). Managing the remediation strategy of contaminated megasites using field-scale calibration of geo-electrical imaging with chemical monitoring. *The Science of the Total Environment*, *920*, 171013. https://doi.org/10.1016/j.scitotenv.2024.171013

Lévy, L., Thalund-Hansen, R., Bording, T., Fiandaca, G., Christiansen, A. V., Rügge, K., et al. (2022). Quantifying reagent spreading by Cross-Borehole electrical tomography to assess performance of groundwater remediation. *Water Resources Research*, *58*(9), e2022WR032218. https://doi.org/10.1029/2022wr032218

Liao, Q., Deng, Y., Shi, X., Sun, Y., Duan, W., & Wu, J. (2018). Delineation of contaminant plume for an inorganic contaminated site using electrical resistivity tomography: Comparison with direct-push technique. *Environmental Monitoring and Assessment*, *190*(4), 187. https://doi.org/10.1007/s10661-018-6560-3

Linde, N., Renard, P., Mukerji, T., & Caers, J. (2015). Geological realism in hydrogeological and geophysical inverse modeling: A review. *Advances in Water Resources*, *86*, 86–101. https://doi.org/10.1016/j.advwatres.2015.09.019

Liu, J., Chen, Q., Yang, Y., Wei, H., Laipan, M., Zhu, R., et al. (2022). Coupled redox cycling of Fe and Mn in the environment: The complex interplay of solution species with Fe- and Mn-(oxyhydr)oxide crystallization and transformation. *Earth-Science Reviews*, *232*, 104105. https://doi.org/10.1016/j.earscirev.2022.104105

Loke, M., & Barker, R. (1996). Rapid least-squares inversion of apparent resistivity pseudosections by a quasi-Newton method[1]. *Geophysical Prospecting*, *44*(1), 131–152. https://doi.org/10.1111/j.1365-2478.1996.tb00142.x

Ma, J., Li, H., Chi, L., Chen, H., & Chen, C. (2017). Changes in activation energy and kinetics of heat-activated persulfate oxidation of phenol in response to changes in pH and temperature. *Chemosphere*, *189*, 86–93. https://doi.org/10.1016/j.chemosphere.2017.09.051

Ma, X., Schwartz, N., Chao, C., Li, J., Xia, T., Furman, A., & Mao, D. (2025). Unveiling spectral induced polarization responses of ZVI-AC-SAND mixtures in groundwater remediation. *Journal of Geophysical Research: Solid Earth*, *130*(3), e2024JB030107. https://doi.org/10.1029/2024jb030107

Ma, X., Zhang, J., Chao, C., Liu, S., Rahman, K. U., Li, S., et al. (2025). Tracking Cr(VI) removal with spectral induced polarization under ZVI and AC synergetic remediation. *Environmental Research*, *267*, 120707. https://doi.org/10.1016/j.envres.2024.120707

Mahmoudi, D., Rezaei, M., Ashjari, J., Salehghamari, E., Jazaei, F., & Babakhani, P. (2020). Impacts of stratigraphic heterogeneity and release pathway on the transport of bacterial cells in porous media. *The Science of the Total Environment*, *729*, 138804. https://doi.org/10.1016/j.scitotenv.2020.138804

Majone, M., Verdini, R., Aulenta, F., Rossetti, S., Tandoi, V., Kalogerakis, N., et al. (2015). In situ groundwater and sediment bioremediation: Barriers and perspectives at European contaminated sites. *New Biotechnology*, *32*(1), 133–146. https://doi.org/10.1016/j.nbt.2014.02.011

Mak, M. S. H., & Lo, I. M. C. (2011). Environmental life cycle assessment of permeable reactive barriers: Effects of construction methods, reactive materials and groundwater constituents. *Environmental Science and Technology*, *45*(23), 10148–10154. https://doi.org/10.1021/es202016d

Marcon, L., Oliveras, J., & Puntes, V. F. (2021). In situ nanoremediation of soils and groundwaters from the nanoparticle's standpoint: A review. *The Science of the Total Environment*, *791*, 148324. https://doi.org/10.1016/j.scitotenv.2021.148324

Marshall, D. J., & Madden, T. R. (1959). Induced polarization, a study of its causes. *Geophysics*, *24*(4), 790–816. https://doi.org/10.1190/1.1438659

Martinho, E. (2023). Electrical resistivity and induced polarization methods for environmental investigations: An overview. *Water, Air, and Soil Pollution*, *234*(4), 215. https://doi.org/10.1007/s11270-023-06214-x

Mellage, A., Holmes, A. B., Linley, S., Vallée, L., Rezanezhad, F., Thomson, N., et al. (2018). Sensing coated iron-oxide nanoparticles with Spectral Induced Polarization (SIP): Experiments in natural sand packed flow-through columns. *Environmental Science and Technology*, *52*(24), 14256–14265. https://doi.org/10.1021/acs.est.8b03686

Mellage, A., Smeaton, C. M., Furman, A., Atekwana, E. A., Rezanezhad, F., & Van Cappellen, P. (2018). Linking Spectral Induced Polarization (SIP) and subsurface microbial processes: Results from sand column incubation experiments. *Environmental Science and Technology*, *52*(4), 2081–2090. https://doi.org/10.1021/acs.est.7b04420

Meng, J., Dong, Y., Xia, T., Ma, X., Gao, C., & Mao, D. (2022). Detailed LNAPL plume mapping using electrical resistivity tomography inside an industrial building. *Acta Geophysica*, *70*(4), 1651–1663. https://doi.org/10.1007/s11600-022-00818-3

Michael, H. A., & Khan, M. R. (2016). Impacts of physical and chemical aquifer heterogeneity on basin-scale solute transport: Vulnerability of deep groundwater to arsenic contamination in Bangladesh. *Advances in Water Resources*, *98*, 147–158. https://doi.org/10.1016/j.advwatres.2016.10.010

Miller, C. R., Routh, P. S., Brosten, T. R., & McNamara, J. P. (2008). Application of time-lapse ERT imaging to watershed characterization. *Geophysics*, *73*(3), G7–G17. https://doi.org/10.1190/1.2907156

Moshe, S. B., & Furman, A. (2022). Real-time monitoring of organic contaminant adsorption in activated carbon filters using spectral induced polarization. *Water Research*, *212*, 118103. https://doi.org/10.1016/j.watres.2022.118103

Mosmeri, H., Tasharrofi, S., Alaie, E., & Hassani, S. S. (2018). *Controlled-release oxygen nanocomposite for bioremediation of benzene contaminated groundwater* (pp. 601–622). Elsevier eBooks. https://doi.org/10.1016/b978-0-12-811033-1.00023-8

Naudet, V., & Revil, A. (2005). A sandbox experiment to investigate bacteria-mediated redox processes on self-potential signals. *Geophysical Research Letters*, *32*(11). https://doi.org/10.1029/2005gl022735

Nie, J., Wang, Q., Han, L., & Li, J. (2024). Synergistic remediation strategies for soil contaminated with compound heavy metals and organic pollutants. *Journal of Environmental Chemical Engineering*, *12*(4), 113145. https://doi.org/10.1016/j.jece.2024.113145

Niu, Q., & Revil, A. (2016). Connecting complex conductivity spectra to mercury porosimetry of sedimentary rocks. *Geophysics*, *81*(1), E17–E32. https://doi.org/10.1190/geo2015-0072.1

Nivorlis, A., Sparrenbom, C., Rossi, M., Åkesson, S., & Dahlin, T. (2024). Multidisciplinary monitoring of an in-situ remediation test of chlorinated solvents. *The Science of the Total Environment*, *922*, 170942. https://doi.org/10.1016/j.scitotenv.2024.170942

Padhye, L. P., Srivastava, P., Jasemizad, T., Bolan, S., Hou, D., Shaheen, S. M., et al. (2023). Contaminant containment for sustainable remediation of persistent contaminants in soil and groundwater. *Journal of Hazardous Materials*, *455*, 131575. https://doi.org/10.1016/j.jhazmat.2023.131575

Patnode, H., & Wyllie, M. (1950). The presence of conductive solids in reservoir rocks as a factor in electric log interpretation. *Journal of Petroleum Technology*, *2*(2), 47–52. https://doi.org/10.2118/950047-g

Pelton, W. H., Rijo, L., & Swift, C. M. (1978). Inversion OF two-DIMENSIONAL resistivity and induced-polarization data. *Geophysics*, *43*(4), 788–803. https://doi.org/10.1190/1.1440854

Personna, Y. R., Ntarlagiannis, D., Slater, L., Yee, N., O'Brien, M., & Hubbard, S. (2008). Spectral induced polarization and electrodic potential monitoring of microbially mediated iron sulfide transformations. *Journal of Geophysical Research*, *113*(G2). https://doi.org/10.1029/2007jg000614

Petiau, G. (2000). Second generation of lead-lead chloride electrodes for geophysical applications. *Pure and Applied Geophysics*, *157*(3), 357–382. https://doi.org/10.1007/s000240050004

Phenrat, T., Saleh, N., Sirk, K., Tilton, R. D., & Lowry, G. V. (2007). Aggregation and sedimentation of aqueous nanoscale zerovalent iron dispersions. *Environmental Science and Technology*, *41*(1), 284–290. https://doi.org/10.1021/es061349a

Qi, Y., & Wu, Y. (2024). Induced polarization of clayey rocks and soils: Non-linear complex conductivity models. *Journal of Geophysical Research: Solid Earth*, *129*(3), e2023JB028405. https://doi.org/10.1029/2023jb028405

Qiang, S., Xie, W., Shi, X., Deng, S., Long, T., Kang, X., et al. (2025). Geoelectrical monitoring of natural attenuation process in an organic contaminated site including artificial insulating films. *Journal of Hydrology*, *663*, 134161. https://doi.org/10.1016/j.jhydrol.2025.134161

Ramirez, A., Daily, W., LaBrecque, D., Owen, E., & Chesnut, D. (1993). Monitoring an underground steam injection process using electrical resistance tomography. *Water Resources Research*, *29*(1), 73–87. https://doi.org/10.1029/92wr01608

Ramirez, A. L., Daily, W. D., & Newmark, R. L. (1995). Electrical resistance tomography for steam injection monitoring and process control. *Journal of Environmental & Engineering Geophysics*, *1*(A), 39–51. https://doi.org/10.4133/jeeg1.a.39

Revil, A., Florsch, N., & Mao, D. (2015). Induced polarization response of porous media with metallic particles — Part 1: A theory for disseminated semiconductors. *Geophysics*, *80*(5), D525–D538. https://doi.org/10.1190/geo2014-0577.1

Revil, A., & Skold, M. (2011). Salinity dependence of spectral induced polarization in sands and sandstones. *Geophysical Journal International*, *187*(2), 813–824. https://doi.org/10.1111/j.1365-246x.2011.05181.x

Romantschuk, M., Lahti-Leikas, K., Kontro, M., Galitskaya, P., Talvenmäki, H., Simpanen, S., et al. (2023). Bioremediation of contaminated soil and groundwater by in situ biostimulation. *Frontiers in Microbiology*, *14*, 1258148. https://doi.org/10.3389/fmicb.2023.1258148

Sakr, M., Agamawi, H. E., Klammler, H., & Mohamed, M. M. (2023). A review on the use of permeable reactive barriers as an effective technique for groundwater remediation. *Groundwater for Sustainable Development*, *21*, 100914. https://doi.org/10.1016/j.gsd.2023.100914

Sanuade, O. A., Arowoogun, K. I., & Amosun, J. O. (2022). A review on the use of geoelectrical methods for characterization and monitoring of contaminant plumes. *Acta Geophysica*, *70*(5), 2099–2117. https://doi.org/10.1007/s11600-022-00858-9

Sarkar, P., Roy, A., Pal, S., Mohapatra, B., Kazy, S. K., Maiti, M. K., & Sar, P. (2017). Enrichment and characterization of hydrocarbon-degrading bacteria from petroleum refinery waste as potent bioaugmentation agent for in situ bioremediation. *Bioresource Technology*, *242*, 15–27. https://doi.org/10.1016/j.biortech.2017.05.010

Sauck, W. A. (2000). A model for the resistivity structure of LNAPL plumes and their environs in sandy sediments. *Journal of Applied Geophysics*, *44*(2–3), 151–165. https://doi.org/10.1016/s0926-9851(99)00021-x

Scanlon, B. R., Fakhreddine, S., Rateb, A., De Graaf, I., Famiglietti, J., Gleeson, T., et al. (2023). Global water resources and the role of groundwater in a resilient water future. *Nature Reviews Earth and Environment*, *4*(2), 87–101. https://doi.org/10.1038/s43017-022-00378-6

Seigel, H. O. (1959). Mathematical formulation and type CURVES for induced polarization. *Geophysics*, *24*(3), 547–565. https://doi.org/10.1190/1.1438625

Sentenac, P., Hogson, T., Keenan, H., & Kulessa, B. (2015). Small scale monitoring of a bioremediation barrier using miniature electrical resistivity tomography. *Journal of Applied Geophysics*, *115*, 24–31. https://doi.org/10.1016/j.jappgeo.2014.11.006

Shao, G. H., Dong, J., Zhang, W. H., Sun, S. F., Li, C. L., & Li, Y. (2025). In situ bioelectrochemical remediation of contaminated soil and groundwater: A review. *Environmental Pollution*, *374*, 126250. https://doi.org/10.1016/j.envpol.2025.126250

Shi, Z., Fan, D., Johnson, R. L., Tratnyek, P. G., Nurmi, J. T., Wu, Y., & Williams, K. H. (2015). Methods for characterizing the fate and effects of nano zerovalent iron during groundwater remediation. *Journal of Contaminant Hydrology*, *181*, 17–35. https://doi.org/10.1016/j.jconhyd.2015.03.004

Singh, R., Chakma, S., & Birke, V. (2023). Performance of field-scale permeable reactive barriers: An overview on potentials and possible implications for in-situ groundwater remediation applications. *The Science of the Total Environment*, *858*, 158838. https://doi.org/10.1016/j.scitotenv.2022.158838

Singha, K., Day-Lewis, F. D., Johnson, T., & Slater, L. D. (2014). Advances in interpretation of subsurface processes with time-lapse electrical imaging. *Hydrological Processes*, *29*(6), 1549–1576. https://doi.org/10.1002/hyp.10280

Slater, L., & Binley, A. (2003). Evaluation of permeable reactive barrier (PRB) integrity using electrical imaging methods. *Geophysics*, *68*(3), 911–921. https://doi.org/10.1190/1.1581043

Slater, L., & Binley, A. (2006). Synthetic and field-based electrical imaging of a zerovalent iron barrier: Implications for monitoring long-term barrier performance. *Geophysics*, *71*(5), B129–B137. https://doi.org/10.1190/1.2235931

Slater, L., & Binley, A. (2021). Advancing hydrological process understanding from long-term resistivity monitoring systems. *Wiley Interdisciplinary Reviews. Water*, *8*(3), e1513. https://doi.org/10.1002/wat2.1513

Slater, L., Choi, J., & Wu, Y. (2005). Electrical properties of iron-sand columns: Implications for induced polarization investigation and performance monitoring of iron-wall barriers. *Geophysics*, *70*(4), G87–G94. https://doi.org/10.1190/1.1990218

Slater, L., & Lesmes, D. (2002). IP interpretation in environmental investigations. *Geophysics*, *67*(1), 77–88. https://doi.org/10.1190/1.1451353

Song, B., Zeng, G., Gong, J., Liang, J., Xu, P., Liu, Z., et al. (2017). Evaluation methods for assessing effectiveness of in situ remediation of soil and sediment contaminated with organic pollutants and heavy metals. *Environment International*, *105*, 43–55. https://doi.org/10.1016/j.envint.2017.05.001

Song, Y., Shi, X., Revil, A., Ghorbani, A., Qiang, S., Xing, K., et al. (2024). Spectral induced polarization response of bacteria growth and decay in soil column experiments. *Journal of Geophysical Research: Biogeosciences*, *129*(12), e2024JG008050. https://doi.org/10.1029/2024jg008050

Song, Y., Shi, X., Revil, A., & Kang, X. (2022). Monitoring in situ microbial growth and decay in soil Column experiments by Induced polarization. *Geophysical Research Letters*, *49*(16), e2021GL097553. https://doi.org/10.1029/2021gl097553

Sparrenbom, C. J., Åkesson, S., Johansson, S., Hagerberg, D., & Dahlin, T. (2017). Investigation of chlorinated solvent pollution with resistivity and induced polarization. *The Science of the Total Environment*, *575*, 767–778. https://doi.org/10.1016/j.scitotenv.2016.09.117

Sturman, P., Stewart, P., Cunningham, A., Bouwer, E., & Wolfram, J. (1995). Engineering scale-up of in situ bioremediation processes: A review. *Journal of Contaminant Hydrology*, *19*(3), 171–203. https://doi.org/10.1016/0169-7722(95)00017-p

Sumner, J. S. (1976). Principles of Induced polarization for geophysical exploration. In *Developments in economic geology* (p. 227). Elsevier. https://doi.org/10.1016/c2009-0-14519-1

Sun, X., Zhao, L., Huang, M., Hai, J., Liang, X., Chen, D., & Liu, J. (2024). In-situ thermal conductive heating (TCH) for soil remediation: A review. *Journal of Environmental Management*, *351*, 119602. https://doi.org/10.1016/j.jenvman.2023.119602

Takata, S., Miele, M., Tyrala, L., & Michelsen, F. (2005). *Cost effective geophysical approaches for various geotechnical problems*. Site characterization and modeling. https://doi.org/10.1061/40785(164)7

Tao, J., Rehman, S. U., Ali, R., & Raza, S. A. (2025). Advancement and challenges: A review of power cable aging monitoring and diagnostic techniques. *Renewable and Sustainable Energy Reviews*, *222*, 115970. https://doi.org/10.1016/j.rser.2025.115970

Tarasov, A., & Titov, K. (2013). On the use of the Cole–Cole equations in spectral induced polarization. *Geophysical Journal International*, *195*(1), 352–356. https://doi.org/10.1093/gji/ggt251

Telford, W. M., Geldart, L. P., & Sheriff, R. E. (1990). Applied geophysics. https://doi.org/10.1017/cbo9781139167932

Thalund-Hansen, R., Troldborg, M., Levy, L., Christiansen, A. V., Bording, T. S., & Bjerg, P. L. (2023). Assessing contaminant mass discharge uncertainty with application of hydraulic conductivities derived from geoelectrical Cross-Borehole induced polarization and other methods. *Water Resources Research*, *59*(8), e2022WR034360. https://doi.org/10.1029/2022wr034360

Thompson, J., Mangel, A., & Day-Lewis, F. D. (2023). A geophysical remediation monitoring method selection tool (GRM-MST). *Ground Water*, *61*(1), 8–10. https://doi.org/10.1111/gwat.13268

Tildy, P., Neducza, B., Nagy, P., Kanli, A. I., & Hegymegi, C. (2017). Time lapse 3D geoelectric measurements for monitoring of in-situ remediation. *Journal of Applied Geophysics*, *136*, 99–113. https://doi.org/10.1016/j.jappgeo.2016.10.037

Tratnyek, P. G., Johnson, R. L., Lowry, G. V., & Brown, R. A. (2014). *IN SITU chemical reduction for source remediation* (pp. 307–351). Springer eBooks. https://doi.org/10.1007/978-1-4614-6922-3_10

Trento, L. M., Tsourlos, P., & Gerhard, J. I. (2021). Time-lapse electrical resistivity tomography mapping of DNAPL remediation at a STAR field site. *Journal of Applied Geophysics*, *184*, 104244. https://doi.org/10.1016/j.jappgeo.2020.104244

Tsakirmpaloglou, K., Martin, T., Kaufmann, O., & Goderniaux, P. (2020). Monitoring system for remediation of a brownfield area. *NSG2021 27th European Meeting of Environmental and Engineering Geophysics*, 1–5. https://doi.org/10.3997/2214-4609.202020167

Tso, C. M., Johnson, T. C., Song, X., Chen, X., Kuras, O., Wilkinson, P., et al. (2020). Integrated hydrogeophysical modelling and data assimilation for geoelectrical leak detection. *Journal of Contaminant Hydrology*, *234*, 103679. https://doi.org/10.1016/j.jconhyd.2020.103679

Tso, C. M., Kuras, O., & Binley, A. (2019). On the field estimation of moisture content using electrical geophysics: The impact of petrophysical model uncertainty. *Water Resources Research*, *55*(8), 7196–7211. https://doi.org/10.1029/2019wr024964

U.S. Army Corps of Engineers (USACE). (2014). Design: In situ thermal remediation. EX 200-1-21. Retrieved from https://clu-in.org/download/techfocus/thermal/Thermal-In-Situ-EM-200-1-21-1.pdf

Vinegar, H. J., & Waxman, M. H. (1984). Induced polarization of Shaly sands. *Geophysics*, *49*(8), 1267–1287. https://doi.org/10.1190/1.1441755

Vogt, C., & Richnow, H. H. (2013). *Bioremediation via in situ microbial degradation of organic pollutants* (pp. 123–146). Biotechnology. https://doi.org/10.1007/10_2013_266

Wang, L., Peng, L., Xie, L., Deng, P., & Deng, D. (2017). Compatibility of surfactants and thermally activated persulfate for enhanced subsurface remediation. *Environmental Science and Technology*, *51*(12), 7055–7064. https://doi.org/10.1021/acs.est.6b05477

Wang, L. W., Rinklebe, J., Tack, F. M. G., & Hou, D. Y. (2021). A review of green remediation strategies for heavy metal contaminated soil. *Soil Use & Management*, *37*(4), 936–963. https://doi.org/10.1111/sum.12717

Wang, Q., Guo, S., Ali, M., Song, X., Tang, Z., Zhang, Z., et al. (2022). Thermally enhanced bioremediation: A review of the fundamentals and applications in soil and groundwater remediation. *Journal of Hazardous Materials*, *433*, 128749. https://doi.org/10.1016/j.jhazmat.2022.128749

Wang, W., Dong, J., & Zhao, H. (2025). In-situ remediation of contaminated groundwater by bioelectrochemical system: A review. *International Biodeterioration and Biodegradation*, *196*, 105914. https://doi.org/10.1016/j.ibiod.2024.105914

Wei, K., Ma, J., Xi, B., Yu, M., Cui, J., Chen, B., et al. (2022). Recent progress on in-situ chemical oxidation for the remediation of petroleum contaminated soil and groundwater. *Journal of Hazardous Materials*, *432*, 128738. https://doi.org/10.1016/j.jhazmat.2022.128738

Weller, A., Slater, L., Binley, A., Nordsiek, S., & Xu, S. (2015). Permeability prediction based on induced polarization: Insights from measurements on sandstone and unconsolidated samples spanning a wide permeability range. *Geophysics*, *80*(2), D161–D173. https://doi.org/10.1190/geo2014-0368.1

Weller, A., Slater, L., & Nordsiek, S. (2013). On the relationship between induced polarization and surface conductivity: Implications for petrophysical interpretation of electrical measurements. *Geophysics*, *78*(5), D315–D325. https://doi.org/10.1190/geo2013-0076.1

Weller, A., Slater, L., Nordsiek, S., & Ntarlagiannis, D. (2010). On the estimation of specific surface per unit pore volume from induced polarization: A robust empirical relation fits multiple data sets. *Geophysics*, *75*(4), WA105–WA112. https://doi.org/10.1190/1.3471577

Williams, K. H., Kemna, A., Wilkins, M. J., Druhan, J., Arntzen, E., N'Guessan, A. L., et al. (2009). Geophysical monitoring of coupled microbial and geochemical processes during stimulated subsurface bioremediation. *Environmental Science and Technology*, *43*(17), 6717–6723. https://doi.org/10.1021/es900855j

Williams, K. H., Ntarlagiannis, D., Slater, L. D., Dohnalkova, A., Hubbard, S. S., & Banfield, J. F. (2005). Geophysical imaging of stimulated microbial biomineralization. *Environmental Science and Technology*, *39*(19), 7592–7600. https://doi.org/10.1021/es0504035

Winsauer, W., & McCardell, W. (1953). Ionic Double-Layer conductivity in reservoir rock. *Journal of Petroleum Technology*, *5*(5), 129–134. https://doi.org/10.2118/953129-g

Wu, N., Zhang, W., Wei, W., Yang, S., Wang, H., Sun, Z., et al. (2020). Field study of chlorinated aliphatic hydrocarbon degradation in contaminated groundwater via micron zero-valent iron coupled with biostimulation. *Chemical Engineering Journal*, *384*, 123349. https://doi.org/10.1016/j.cej.2019.123349

Wu, Q., Sun, Y., Luo, Z., Li, X., Wen, Y., Shi, Y., et al. (2024). Application and development of zero-valent iron (ZVI)-based materials for environmental remediation: A scientometric and visualization analysis. *Environmental Research*, *241*, 117659. https://doi.org/10.1016/j.envres.2023.117659

Wu, Y. X., Slater, L., Versteeg, R., & LaBrecque, D. (2008). A comparison of the low frequency electrical signatures of iron oxide versus calcite precipitation in granular zero valent iron columns. *Journal of Contaminant Hydrology*, *95*(3–4), 154–167. https://doi.org/10.1016/j.jconhyd.2007.09.003

Wu, Y. X., Slater, L. D., & Korte, N. (2005). Effect of precipitation on low frequency electrical properties of zerovalent iron columns. *Environmental Science and Technology*, *39*(23), 9197–9204. https://doi.org/10.1021/es051052x

Wu, Y. X., Slater, L. D., & Korte, N. (2006). Low frequency electrical properties of corroded iron barrier cores. *Environmental Science and Technology*, *40*(7), 2254–2261. https://doi.org/10.1021/es0520868

Wu, Y. X., Versteeg, R., Slater, L., & LaBrecque, D. (2009). Calcite precipitation dominates the electrical signatures of zero valent iron columns under simulated field conditions. *Journal of Contaminant Hydrology*, *106*(3–4), 131–143. https://doi.org/10.1016/j.jconhyd.2009.02.003

Xia, T. (2025). Data for "the evolving roles of electrical geophysical methods for in situ remediation assessment: Progress and perspectives [Dataset]. *Zenodo*. https://zenodo.org/records/17971362

Xia, T., Huisman, J. A., Chao, C., Li, J., & Mao, D. (2025). Induced polarization monitoring of in-situ chemical oxidation for quantification of contaminant consumption. *Journal of Contaminant Hydrology*, *269*, 104481. https://doi.org/10.1016/j.jconhyd.2024.104481

Xia, T., Ma, M., Huisman, J. A., Zheng, C., Gao, C., & Mao, D. (2023). Monitoring of in-situ chemical oxidation for remediation of diesel-contaminated soil with electrical resistivity tomography. *Journal of Contaminant Hydrology*, *256*, 104170. https://doi.org/10.1016/j.jconhyd.2023.104170

Xia, T., Meng, J., Ding, B., Chen, Z., Liu, S., Titov, K., & Mao, D. (2023). Integration of hydrochemical and induced polarization analysis for leachate localization in a municipal landfill. *Waste Management*, *157*, 130–140. https://doi.org/10.1016/j.wasman.2022.12.014

Xia, T., Zhang, J., Guo, L., Li, S., Ma, X., & Mao, D. (2023). Dynamic monitoring of In-situ chemical oxidation for remediation of hydrocarbon contamination with electrical resistivity tomography. *Journal of Physics Conference Series*, *2651*(1), 012105. https://doi.org/10.1088/1742-6596/2651/1/012105

Xia, T., Zhang, J., Li, M., Jougnot, D., Yang, K., Li, S., & Mao, D. (2025). Evolution of in-situ thermal-enhanced oxidative remediation monitored by induced polarization tomography. *Journal of Hydrology*, *648*, 132464. https://doi.org/10.1016/j.jhydrol.2024.132464

Xia, T., Zhang, J., Li, M., Li, S., Guo, L., Liu, P., et al. (2025). Towards efficient in situ gas thermal desorption remediation assisted with cross-borehole resistivity tomography. *Water Research*, *281*, 123587. https://doi.org/10.1016/j.watres.2025.123587

Xu, X., Hu, N., Wang, Q., Li, X., Yu, Z., Song, X., & Fan, L. (2024). Insights into the relationship between temperature variation and NAPL removal during in situ thermal remediation of soil in the presence of NAPL–Water Co-boiling: A two-dimensional visualized sandbox Study. *Environmental Science and Technology*, *58*(51), 22594–22602. https://doi.org/10.1021/acs.est.4c09388

Yang, Y., Zhou, S., Luo, Y., Chen, J., Chen, Z., Cao, J., et al. (2024). Monitoring the remediation of groundwater polluted by MSW landfill leachates by activated carbon and zeolite with spectral induced polarization technique. *Environmental Geochemistry and Health*, *46*(1), 1. https://doi.org/10.1007/s10653-023-01796-1

Yuan, L., Wang, K., Zhao, Q., Yang, L., Wang, G., Jiang, M., & Li, L. (2024). An overview of in situ remediation for groundwater co-contaminated with heavy metals and petroleum hydrocarbons. *Journal of Environmental Management*, *349*, 119342. https://doi.org/10.1016/j.jenvman.2023.119342

Zehe, E., Loritz, R., Edery, Y., & Berkowitz, B. (2021). Preferential pathways for fluid and solutes in heterogeneous groundwater systems: Self-organization, entropy, work. *Hydrology and Earth System Sciences*, *25*(10), 5337–5353. https://doi.org/10.5194/hess-25-5337-2021

Zhang, C., Revil, A., Fujita, Y., Munakata-Marr, J., & Redden, G. (2014). Quadrature conductivity: A quantitative indicator of bacterial abundance in porous media. *Geophysics*, *79*(6), D363–D375. https://doi.org/10.1190/geo2014-0107.1

Zhang, S., Mao, G., Crittenden, J., Liu, X., & Du, H. (2017). Groundwater remediation from the past to the future: A bibliometric analysis. *Water Research*, *119*, 114–125. https://doi.org/10.1016/j.watres.2017.01.029

Zhang, T., Lowry, G. V., Capiro, N. L., Chen, J., Chen, W., Chen, Y., et al. (2019). In situ remediation of subsurface contamination: Opportunities and challenges for nanotechnology and advanced materials. *Environmental Science: Nano*, *6*(5), 1283–1302. https://doi.org/10.1039/c9en00143c

Zhang, X., Nawaz, M. A., Zhao, X., & Curtis, A. (2021). An introduction to variational inference in geophysical inverse problems. *Advances in Geophysics*, 73–140. https://doi.org/10.1016/bs.agph.2021.06.003

Zhang, Y., Labianca, C., Chen, L., De Gisi, S., Notarnicola, M., Guo, B., et al. (2021). Sustainable ex-situ remediation of contaminated sediment: A review. *Environmental Pollution*, *287*, 117333. https://doi.org/10.1016/j.envpol.2021.117333

Zhang, Y., Zhang, C., Xu, J., Li, L., Li, D., Wu, Q., & Ma, L. (2022). Strategies to enhance the reactivity of zero-valent iron for environmental remediation: A review. *Journal of Environmental Management*, *317*, 115381. https://doi.org/10.1016/j.jenvman.2022.115381

Zhao, B., Sun, Z., & Liu, Y. (2022). An overview of in situ remediation for nitrate in groundwater. *The Science of the Total Environment*, *804*, 149981. https://doi.org/10.1016/j.scitotenv.2021.149981